



Effects of Microbial-Mineral Interactions on Organic Carbon Stabilization in a Ponderosa Pine Root Zone: A Micro-Scale Approach

Alice C. Dohnalkova^{1*}, Malak M. Tfaily^{1,2}, Rosalie K. Chu¹, A. Peyton Smith³, Colin J. Brislawn⁴, Tamas Varga¹, Alex R. Crump⁵, Libor Kovarik⁶, Linda S. Thomashow⁷, James B. Harsh⁸, C. Kent Keller⁹ and Zsuzsanna Balogh-Brunstad¹⁰

¹Environmental Molecular Sciences Laboratory, Pacific Northwest National Laboratory, Richland, WA, United States, ²Department of Environmental Science, University of Arizona, Tucson, AZ, United States, ³Soil and Crop Sciences, Texas A&M AgriLife, College Station, TX, United States, ⁴Biological Sciences Division, Pacific Northwest National Laboratory, Richland, WA, United States, ⁵Department of Soil and Water Systems, University of Idaho, Moscow, ID, United States, ⁶Physical & Computational Sciences Directorate, Pacific Northwest National Laboratory, Richland, WA, United States, ⁷USDA-ARS, Wheat Health, Genetics and Quality Research Unit, Washington State University, Pullman, WA, United States, ⁸Department of Crop & Soil Sciences, Washington State University, Pullman, WA, United States, ⁹School of the Environment, Washington State University, Pullman, WA, United States, ¹⁰Department of Geology and Environmental Sciences, Hartwick College, Oneonta, NY, United States

OPEN ACCESS

Edited by:

Andrew C. Mitchell,
Aberystwyth University,
United Kingdom

Reviewed by:

Olubukola Oluranti Babalola,
North-West University, South Africa
Kenneth Hurst Williams,
Berkeley Lab (DOE), United States

*Correspondence:

Alice C. Dohnalkova
Alice.dohnalkova@pnl.gov

Specialty section:

This article was submitted to
Geochemistry,
a section of the journal
Frontiers in Earth Science

Received: 21 October 2021

Accepted: 06 May 2022

Published: 24 May 2022

Citation:

Dohnalkova AC, Tfaily MM, Chu RK, Smith AP, Brislawn CJ, Varga T, Crump AR, Kovarik L, Thomashow LS, Harsh JB, Keller CK and Balogh-Brunstad Z (2022) Effects of Microbial-Mineral Interactions on Organic Carbon Stabilization in a Ponderosa Pine Root Zone: A Micro-Scale Approach. *Front. Earth Sci.* 10:799694. doi: 10.3389/feart.2022.799694

Soil microbial communities affect the formation of micro-scale mineral-associated organic matter (MAOM) where complex processes, including adhesion, aggregate formation, microbial mineral weathering and soil organic matter stabilization occur in a narrow zone of large biogeochemical gradients. Here we designed a field study to examine carbon stabilization mechanisms by using in-growth mesh bags containing biotite that were placed in a ponderosa pine root zone for 6 months and compared to the surrounding bulk soil. We sought to determine the composition of the microbial community in the mesh bags compared to the surrounding soils, analyze the direct interactions between microbes and biotite, and finally identify the nature of the newly formed MAOM within the mesh-bags. Our results revealed that minerals in the mesh bags were colonized by a microbial community that produced organic matter *in situ*. The 16S rRNA gene sequencing and ITS2 region characterization showed phylogenetic similarity between the mesh bag and bulk soil archaea/bacteria and fungi microbiomes, with significant differences in alpha- and beta-diversity and species abundances. Organic matter pools in the mesh bags, analyzed by Fourier transform ion cyclotron resonance mass spectrometry, contained protein-(peptides) and lipid-like compounds while the bulk soil OM was comprised of lignin-like and carboxyl-rich alicyclic molecules. These results support that the newly formed biotite associated organic compounds have a microbial signature in the mesh bags. High-resolution electron microscopy documented strongly adhered organic compounds to biotite surfaces, formation of microaggregates, elemental uptake at the microbe (organic matter)-mineral interface, and distortion of biotite layers. Overall, this study shows the direct and indirect involvement of soil microbial communities from the root zone of ponderosa pine in the formation of MAOM, soil organic carbon stabilization, microaggregation, and mineral weathering at micro- and nano-scales.

Keywords: MAOM, mineral weathering, soil organic carbon, electron microscopy, biotite, fourier-transform ion cyclotron resonance mass spectrometry

1 INTRODUCTION

Interactions between microorganisms and soil particles are highly complex. These processes include microbial adhesion to a mineral substrate and formation of mineral-associated organic matter (MAOM) (Lavallee et al., 2020; Olayemi et al., 2022). Microbes also facilitate electron transfer with mineral surfaces (Gorby et al., 2006), enhance mineral weathering (Banfield, 1997; Uroz et al., 2009) and cation acquisition in association with plants (Dontsova et al., 2020), and play a significant role in secondary mineral formation, aggregation, decomposition, and stabilization of soil organic matter (SOM) (Phillips et al., 2014; Shah et al., 2016; Angst et al., 2021; Kleber et al., 2021). Organic carbon enters the soil as aboveground and belowground plant material, microbial biomass and necromass, and exudates from plant roots and fungal hyphae (Liang et al., 2019; Sokol and Bradford, 2019; Angst et al., 2021). It has been postulated that all soil carbon that forms SOM is originally processed by soil microorganisms regardless of its source, and that organic matter “must decay in order to release the energy and nutrients that drive living processes all over the planet” (Janzen, 2006). However, plant material and biomolecules could account for up to half of the stabilized SOM in soil aggregates and MAOM (Angst et al., 2021). In the face of global climate change, questions arise about how to increase stabilization of organic matter and long-term carbon storage in soils (Qafoku, 2015) as part of a strategy for mitigating the impact of climate change (Lehmann et al., 2020). Thus, understanding of the dynamics of SOM and its interactions with minerals in soil environments is crucial.

Aggregate and microaggregate formation is one way to decrease SOM decomposition rates and stabilize organic carbon (Angst et al., 2021; Ozlu and Arriaga, 2021). Microaggregates are composite soil structures that are smaller than 250 μm (Totsche et al., 2018) and include colloidal and nanoparticle mixed phases and organo-mineral components (Chenu and Plante, 2006; Totsche et al., 2018). Spatial inaccessibility rather than solely chemical composition is considered the main reason for increased residence times of SOM in aggregates (Lehmann and Kleber, 2015), but other protection mechanisms such as occlusion, intercalation, hydrophobicity and encapsulation also are contemplated (von Lutzow et al., 2006; Kaiser and Guggenberger, 2007). Soil microorganisms produce extracellular polymeric substances (EPS) that can control bacterial flocculation, biofilm formation and cell adhesion to solid surfaces (Korenevsky and Beveridge, 2007). The adhesion of EPS to minerals and its “cementing” capacity play an important role in the formation of MAOM, and ultimately, of soil aggregates. This subject has been extensively reviewed (Jastrow et al., 1998; Kogel-Knabner et al., 2008; Kleber et al., 2015). In addition, EPS binds metal ions, entraps mineral fragments, aids dissolution-precipitation and colloid transport (Fredrickson and Fletcher, 2001), and results in precipitation of salts *via* dehydration (Dohnalkova et al., 2011). Bacterial EPS can

also influence mineral oxidation/reduction (Fredrickson and Fletcher, 2001), as it is an important component of microbes’ extended electron transfer system. Under conditions of electron acceptor limitation, EPS can evolve into electron-conducting nanowires to facilitate extracellular electron transfer (Gorby et al., 2006) and actively change the soil environment.

Carbon dynamics in the soil environment has been linked to another essential role of microorganisms, the chemical weathering of minerals. The release of key inorganic nutrients from minerals is required not only for growth and sustenance of the microbes but also for that of plants and other living organisms. Mineral composition can influence the microbial community and promote colonization by specifically adapted microbes with mineral-weathering abilities (Hutchens et al., 2010; Uroz et al., 2015). In ecosystems with low non-nitrogen nutrient availability, diverse genera of bacteria can facilitate mineral weathering (Banfield, 1997; Uroz et al., 2009), often forming complex microbial communities with fungi that colonize mineral surfaces (Hutchens, 2009; Kandeler et al., 2019; Colin et al., 2021). However, few studies of microbial weathering have combined both functional and taxonomic investigations for these environments (Lepleux et al., 2012; Kelly et al., 2016; Colin et al., 2017; Whitman et al., 2018). In these studies, the mineral-associated bacterial communities differed significantly from those of the surrounding bulk soil, and bacteria of only certain classes colonized a particular mineral type, depending on their ability to access and mobilize certain cations.

Mycorrhizal fungi are known to mostly use labile carbon received from the host plants for their energy requirements and in exchange for mineral-driven nutrients (Soudzilovskaia et al., 2019), while saprophytic fungi are documented to breakdown large and “recalcitrant” organic molecules such as lignin and cellulose (Kubartova et al., 2009; Janusz et al., 2017). Thus, saprophytic fungi have a significant function in SOM dynamics, especially in forested ecosystems (Kubartova et al., 2009). Numerous studies have demonstrated the essential function of mycorrhizal fungi in mineral weathering and inorganic nutrient uptake that has been fueled by plant-driven carbon allocation and governed by nutrient and water availability (Phillips et al., 2014; Dontsova et al., 2020; Finlay et al., 2020; Li et al., 2021). However, the role of mycorrhizal fungi is poorly understood in SOM turnover and stabilization even though mineral weathering processes directly create fungi-mineral interactions, facilitating organo-mineral associations, adhesion of organic matter to mineral surfaces, formation of MAOM, influencing the redox states of metal ions in the mineral lattice, and liberating cations from mineral structure (Courty et al., 2010; Phillips et al., 2014). It has been documented that (ecto) mycorrhizal fungi directly forage SOM to supply nitrogen to their host plants. Nitrogen and carbon ratios of SOM influence the effectiveness of ectomycorrhizal fungal foraging (Makarov, 2019; Kopittke et al., 2020). In addition, it has been observed that mycorrhizal fungi indirectly increase the breakdown of “old”

recalcitrant SOM by exuding the plant-supplied labile carbon into the rhizosphere, which can act as a priming agent for decomposition (Jackson et al., 2019). This finding indicates that there are no distinct long-term recalcitrant pools of SOM; rather, the pools comprise a continuum in the soil environment (Lehmann and Kleber, 2015).

An increased understanding of the complexity and connectedness of these interactions among microorganisms, SOM, and minerals has been developing with the analytical advances in -omics technologies (White et al., 2017), and development of chemical imaging tools and novel approaches in modeling (Lawrence et al., 2009; Wieder et al., 2013; Wieder et al., 2014). Chemical imaging, stable isotope probing (Pett-Ridge and Firestone, 2017), coupled with X-ray spectromicroscopy (Keiluweit et al., 2012; Chen et al., 2014), atomic resolution imaging and chemical analysis (Dohnalkova et al., 2017; Newcomb et al., 2017; Possinger et al., 2020) have brought new perspectives on MAOM (Kogel-Knabner et al., 2008; Kleber et al., 2015; 2021). The heterogeneity and functional complexity of SOM and the temporal and spatial variations of molecular diversity and composition found in soil environments call for interdisciplinary holistic approaches, systematic and targeted investigations, and novel modeling efforts to further understand the mechanism of organo-mineral interactions (Lehmann et al., 2020; Kleber et al., 2021).

Mineral-filled mesh bags incubated in soils have been used for studies of mineral weathering rates by mycorrhizal fungi and associated microbes (Wallander et al., 2006; Turpault et al., 2009). These mesh bags exclude roots, but allow fungal hyphae and soil microbes to enter into the bags and get established, thus isolating their effects in space and time. In this mesh bag study, our goals are to determine and describe the role of ectomycorrhizal fungi and associated microbes on soil carbon dynamics and formation of MAOM in relation to biotite weathering in the root zone of ponderosa pine. Specifically, we contrast the composition of the microbial community in the mesh bags and in the surrounding soil, analyze the direct interactions between microbes and biotite, and identify the newly formed MAOM within the mesh bags. “We hypothesize that 1) biotite in the mesh bags promotes colonization by specifically adapted microbes; 2) the composition of the newly formed mineral (biotite)-associated organic matter in the mesh bags has a signature of microbial activity; and 3) the SOM, microbial biopolymers, and adhered microbes and fungal hyphae cause physicochemical changes as a sign of biogenic mineral weathering.” To test these hypotheses, we combined molecular analyses, high resolution chemical imaging and surface analysis, and X-ray diffraction (XRD) to analyze the content of the mesh bags and the surrounding bulk soil after 6 months of incubation in the root zone of ponderosa pine.

2 MATERIALS AND METHODS

2.1 Experimental Design

In-growth mesh bags containing biotite were placed in a forest with a predominant population of Ponderosa pine (*Pinus ponderosa*) in Central Cascades, WA, United States (N47 44.322; W120 39.494, elevation 606 m). The area is

dominated by hot and dry summers and cold snowy winters. The wet season is from October to March, with an average annual precipitation of 55–65 cm (according to Western Regional Climate Center <https://wrcc.dri.edu/summary/Climsmwa.html>). The soil of the research area is Nard silt loam (Natural Resources Conservation Service, United States Department of Agriculture <http://websoilsurvey.sc.egov.usda.gov/>), which is characterized as well-drained, contains less than 50% sand, less than 25% clay and the remainder are silt particles. The parent material is a combination of sandstone colluvium, loess and volcanic ash. The measured soil pH was 6.20 (± 0.15) at the depth of the experiment, 15 cm below surface.

Biotite [(Ca_{0.16}, K_{1.53}) (Mg_{2.89}, Fe_{2.34}, Al_{0.53}, Ti_{0.24}) (Si_{6.16}, Al_{1.37}) O₂₀ (OH)₂]; WARD's, Rochester, NY, United States) was selected for our *in-situ* study to gain more insight about interactions between biotite and the soil microbiome. This biotite was tested for its weathering ability by mycorrhizal fungi and associated bacteria in laboratory experiments conducted by our research group (Shi et al., 2014; Balogh-Brunstad et al., 2017). Several studies documented that biotite weathering rates are influenced by parameters such as, pH, organic ligands, microorganisms, fungi, particle size, and source rock (Acker and Bricker, 1992; Kalinowski and Schweda, 1996; Balogh Brunstad et al., 2008; Bray et al., 2014; Bray et al., 2015), but biotite remains the key source of nutrients (potassium, iron, and magnesium) in soils and freshly exposed rocks (Bray et al., 2015). Mycorrhizal fungi are able to preferentially take up nutrients from biotite, and create etched, channel like features on its basal planes after a short exposure (Bonneville et al., 2011; Bonneville et al., 2016; Dontsova et al., 2020). However, field studies have shown some contradicting results. Alterations and elemental uptake were documented after exposure to the soil environment (Wallander et al., 2006; Dontsova et al., 2020), but biotite was not preferred by fungi in all forest soils (Rosenstock et al., 2016; Finlay et al., 2020). Thus, biotite seemed to be a good choice for a further study.

The mesh bags were constructed following (Wallander et al., 2001), with modifications. In brief, biotite was ground, and the 100 μm size fraction was separated *via* dry sieving. Biotite particles were sonicated in deionized (DI) water, then rinsed five times with DI water to remove small, adhered particles and dried at 90°C prior to use. One gram of biotite mixed with 1 g of clean quartz (Lane Mountain Company, Valley, WA, United States) was placed into nylon bags (50 μm mesh size) 3 \times 3 cm in size, and heat-sealed under sterile conditions. Adding quartz, an inert mineral, ensured that the mesh bag content mimicked the permeability of the soil, thus, allowed water infiltration. The mesh size allowed entry of the microbial community and fungal hyphae, but not that of roots. Six mesh bags were positioned in the root zone of young ponderosa pine seedlings located within an approximate area of 100 m². The estimated age of the seedlings was 5 years. Placing the mesh bags into the root zone of a known ectomycorrhizal fungal host, ponderosa pine, maximized the chances of colonization by ectomycorrhizal fungi and their associated microbes, and allowed us to examine their role in SOM turnover and stabilization. The mesh bags were oriented horizontally approximately 15 cm below the surface at the

interface between the A and B mineral soil horizons within the root zone of the pine trees. After 6 months of incubation (October to April wet season), the bags were gently removed and processed to characterize the microbial community and newly formed MAOM. The six mesh bags looked identical macroscopically, thus, we selected three of them as representative samples for further analyses described below. Bulk soil was collected in about 20 cm radius around the root zone area where mesh bags were located and combined into a composite sample. Three technical replicates from each mesh bag and the bulk soil samples were prepared for analytical work. Abiotic controls were prepared by placing a mesh bag with 1 g of biotite in a glass container and adding 5 ml of DI. Three closed containers were incubated 15 cm below ground on a site alongside the mesh bags and analyzed at the same as the biotic samples. Additionally, an original (unburied) mesh bag was kept in the lab as a control.

2.2 Microbial Community Analysis

Microbial diversity and community composition in three mesh bags and the surrounding bulk soil were determined by 16S rRNA and ITS amplicon sequencing and subsequent taxonomic analysis. Microbial DNA was extracted using a MoBio PowerSoil[®] DNA Isolation Kit (MoBio Laboratories, Inc., Carlsbad, CA, United States) following the manufacturer's instructions. Eluted DNA was quantified with a QuBit[®] 2.0 Fluorometer and a QuBit[®] dsDNA HS (high sensitivity) Assay Kit (Invitrogen, Carlsbad, CA, United States). The quality of the bacterial DNA product was checked by PCR amplification of the V4 region of the 16S rRNA gene (515f-806r). Fungal DNA product was checked by PCR amplification of the ITS1 region (ITS1f-ITS2). PCR was done with a Taq PCR Master Mix Kit (Qiagen, Hilden, GA, United States) and a DNA Engine Tetrad 2 Peltier thermocycler (Bio Rad, Hercules, CA, United States). PCR conditions and details pertaining to the 16S and ITS primer sets are described in (Caporaso et al., 2012) and (White et al., 1990), respectively. Eluted DNA was stored at -20°C and subsamples (20 μL) from each biological replicate were sent to Argonne National Laboratory (ANL) for sequencing on the Illumina HiSeq2000.

Reads were demultiplexed, joined, and quality filtered using *ea-utils* (Aronesty, 2011), then analyzed with QIIME (Caporaso et al., 2010). VSEARCH (Rognes et al., 2016), an optimal, open-source implementation of USEARCH, was used to dereplicate, sort by abundance, remove single reads, and cluster at 97% identity. The UCHIME algorithm as implemented in VSEARCH was used to check these clusters for chimeras and construct an abundance table by mapping labeled reads to chimera-checked clusters (Edgar et al., 2011). Taxonomy was assigned to the centroid of each operational taxonomic unit (OTU) by finding the last common ancestor of the top three hits to the Greengenes database (McDonald et al., 2012).

2.3 Organic Matter Extracts Analysis by Fourier Transform Ion Cyclotron Resonance Mass Spectrometry

A 12-T Bruker Solarix FTICR mass spectrometer (Bruker Daltonics, Billerica, MA, United States) was used to collect high-mass resolution and mass accuracy spectra of free and

loosely/weakly bound organic molecules in the material from three mesh bags and adjacent bulk soil. The material was extracted sequentially by two solvents with decreasing polarity: in water (Optima[®] LC/MS grade, Fisher Scientific, Suwanee, GA, United States) and 100% methanol (Optima[®] HPLC grade, Fisher Scientific, Suwanee, GA, United States), according to (Tfaily et al., 2017). Samples (0.4 g) were weighed for extraction and then gently shaken sequentially for 30 min in each solvent before being spun down and the supernatant was injected onto the Fourier Transform Ion Cyclotron Resonance Mass Spectrometry (FTICR-MS) instrument outfitted with a standard electrospray ionization (ESI) interface. The spectra were collected in negative ion mode. Water-extracted samples were diluted 1:2 with methanol and methanol-extracted samples were infused directly using a 250 μL Hamilton syringe at a flow rate of 3 $\mu\text{L}/\text{min}$. The coated glass capillary temperature was set to 180°C and the electrospray voltage set to $+4.3\text{ kV}$ or -4.3 kV . The ESI signal was allowed to stabilize for 5 min and data were collected from 100 to 1,300 m/z , resolution was $4.5\text{E}5$ at 451 Da, ion accumulation time was 0.1 s for 96 scan averages co-added, time of flight was set to 0.65 ms, and Q1 was set to 100 m/z . The syringe was then flushed with 50/50 (v/v) methanol/water to prepare for the next sample. Spectra were calibrated by two internal series of dissolved organic matter homologous series separated by 14 Da ($-\text{CH}_2$ groups) and the mass accuracy was calculated to be $<1\text{ ppm}$ for singly charged ions ranging across the mass spectra distribution. Molecular formula assignments were made using a modified version of the Compound Identification Algorithm (CIA) (Kujawinski and Behn, 2006). Spectra from water-extracted samples were selective for carbohydrates with high O:C ratios, whereas spectra from methanol-extracted samples were selective for compounds with low O:C ratios (O:C < 0.5), as established by (Kujawinski et al., 2009). The van Krevelen diagrams were constructed using the elemental oxygen-to-carbon ratio (O/C ratio) on the x-axis and hydrogen to carbon (H/C ratio) on the y-axis. Major biogeochemical classes of compounds (such as lignin-like compounds, lipid-like compounds, etc.) have their own characteristic H/C or O/C ratios. As a result, each class of compounds plots in a specific location on the diagram (Kim et al., 2003).

2.4 Statistical Analysis

Phylogeny data were processed in R by using the Phyloseq package (McMurdie and Holmes, 2013). Samples with less than 10 k reads were removed and remaining samples were rarefied to an even depth. To visualize taxonomy composition, identified microbes were merged at the Class or Family levels, samples were merged by cohort, and only the most abundant microbes are shown. For statistical modeling, unmerged samples and normalized, unmerged OTUs were used.

Residual maximum likelihood (REML) models, a mixed-effect approach, were used to test for differences between sample locations (i.e., bulk soil vs. mesh bag) for the relative abundance of the eleven most abundant classes of bacteria and fungi identified by using 16S (bacterial) and ITS (fungal) sequencing. Field tree was incorporated as a random variable, whereas sample location, month, and their interaction, were fixed

effects. All REML models were run in JMP Version 13.0 (SAS Inst. Inc., Cary, NC, United States).

To test for relationships between 16S, ITS and FTICR data, we performed a nonmetric multi-dimensional scaling (NMS) of Bray-Curtis similarities using combined 16S and ITS data (relative abundance of all identified OTUs merged at the class-rank) as the primary matrix and relative abundance of FT-ICR elemental and compound classes as the secondary matrix using PC-ORD 6 (MjM Software Design, Gleneden Beach, OR, United States). Lipid-, protein- and unsaturated hydrocarbon-like compounds, and CHO compounds with P or S, as well as CHON compounds (including CHONS, CHONP and CHONSP) and amino sugar-, carbohydrate- and condensed hydrocarbon-like compounds were evaluated for association with material from inside the mesh bags and with bulk soil.

2.5 Microbial-Mineral Associations and Mineral-Associated Organic Matter Imaging and Analysis

2.5.1 Scanning Electron Microscopy and Helium Ion Microscopy

The micro- and nano-topography of biotite from mesh bags was inspected using Scanning Electron Microscopy (SEM) and Helium Ion Microscopy (HeIM), with emphasis on visualizing organic matter and microbial attachment to mineral surfaces. Mineral material from the same three samples as for the FTICR was air-dried, then mounted on carbon tape-covered aluminum SEM stubs (Ted Pella, Redding, CA, United States) and sputter-coated with 20 nm of carbon. The mineral particles were imaged with a Helios NanoLab DualBeam SEM (FEI, Hillsboro, OR, United States) at 2 KeV coupled with energy-dispersive X-ray spectroscopy (EDS) operated at 20 keV, and data were analyzed with INCA software (Oxford Instruments). Additionally, samples containing microbial material were imaged with a high-resolution Orion HeIM, (Zeiss, Peabody, MA, United States) at 30 keV.

2.5.2 Transmission Electron Microscopy and Energy Dispersive Spectroscopy

To visualize direct microbial—mineral associations at high resolution and provide their chemical maps, whole mounts of the material were prepared. A 5- μ L drop of water with material from either the mesh bags or the bulk soil was applied to a 100-mesh Cu grid covered with formvar support film sputtered with carbon (Electron Microscopy Sciences, Hatfield, PA, United States). The material was allowed to adhere to the grid for 1 min before the liquid was gently blotted and air-dried. Samples were examined with a Tecnai T-12 transmission electron microscopy (TEM) (FEI) operating at 120 kV with a LaB6 filament. Images were collected digitally with a 2×2 K Ultrascan CCD (Gatan). For cross-sectional TEM, material was processed and embedded in plastic (**Supplementary Table S1**) and sectioned at 70 nm ultrathin sections (Leica Ultracut UCT ultramicrotome, Leica). The sections were mounted on a TEM grid as above and imaged on a Tecnai T-12 TEM. For atomic-resolution imaging and chemical mapping, the material

was applied as a whole mount on an UltraThin C grid (Ted Pella, Redding, CA, United States), and imaged and analyzed with an aberration corrected FEI Titan 80–300 scanning transmission electron microscope (STEM) operated in S/TEM mode using a high angle annular dark field (HAADF) detector. The probe convergence angle was set to 18 mrad and the inner detection angle on the HAADF detector was set to 52 mrad. The elemental analysis was performed using EDS at high collection angle silicon drift detector (~ 0.7 srad, JEOL Centurio). Acquisition and evaluation of the spectra was performed by NSS Thermo Scientific software package.

2.5.3 X-Ray Diffraction Analysis of Minerals

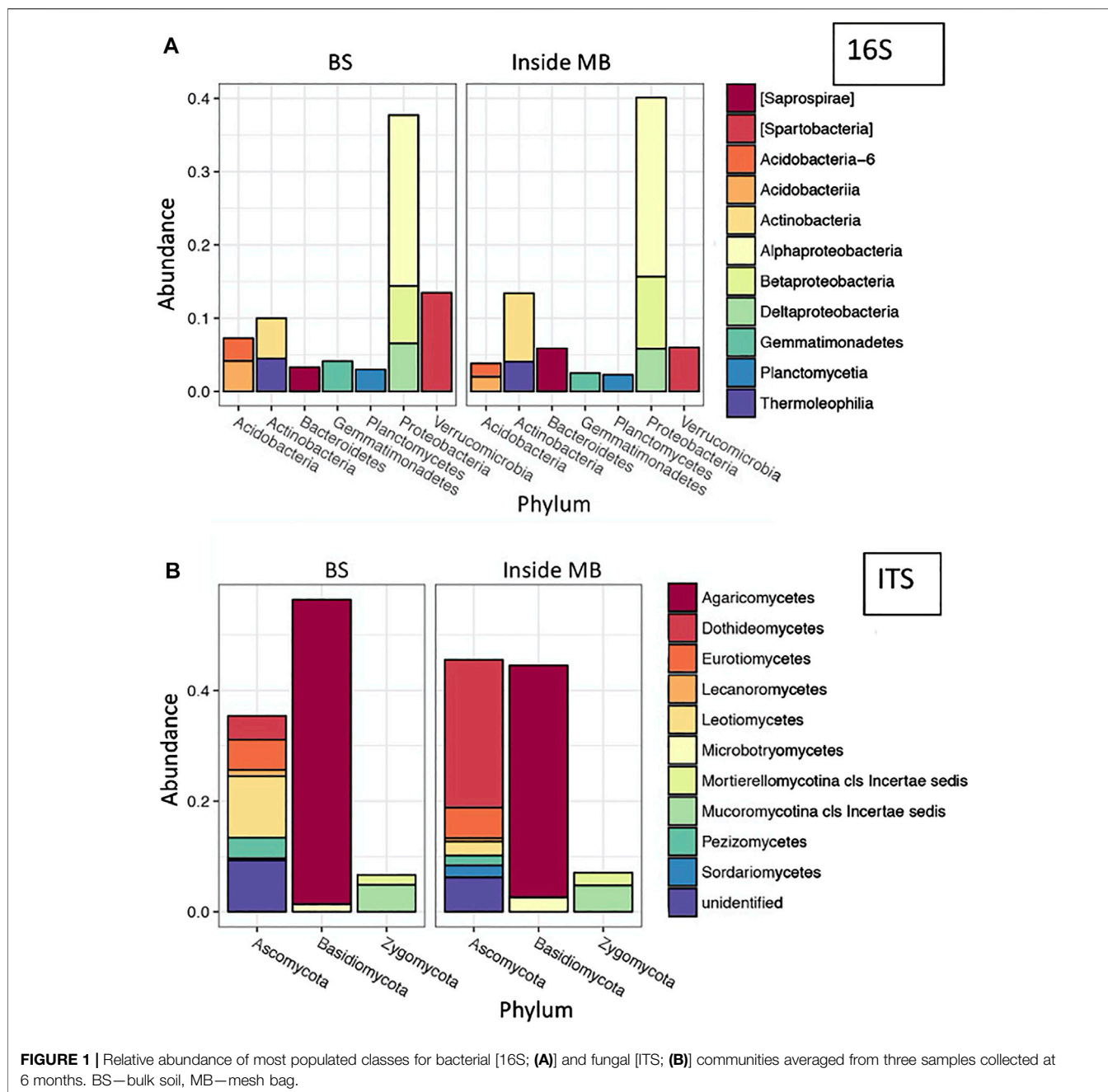
Mineral composition of bulk soil, changes in crystallinity of biotite in mesh bags and formation of amorphous content were examined by using powder-XRD and micro-XRD. A 0.5 g portion of the same three samples used for the FTICR analysis and electron microscopy imaging was homogenized into fine powder by dry grinding and loaded into 0.5-mm-diameter quartz capillaries (Charles Supper Co., Natick, MA, United States) for micro-XRD (Rigaku D/Max Rapid II with a 2D image plate detector) measurements. Change of crystallite sizes of biotite in mesh bags was calculated from Rietveld refinement of the XRD data using the program TOPAS (version 5, Bruker AXS, Germany). For the determination of amorphous content of the samples, a known amount of high-crystallinity corundum internal standard was mixed into the samples and was calculated following Madsen and Scarlett (2008). Detailed description of XRD methods and data analysis are found in Supplementary material.

3 RESULTS

3.1 Microbial Community Composition

To address our hypothesis that biotite in the mesh bags promotes colonization by specifically adapted microbes, we compared the composition of the microbial communities recovered from the bulk soil and the biotite -containing mesh bags. After 6 months, both the bacterial and fungal communities differed between the bulk soil and material extracted from three biological replicates (**Figure 1**). Biotite inside the bags contained more Saprospirea ($p = 0.0350$) and Betaproteobacteria ($p = 0.0225$) than the bulk soil communities, whereas Acidobacteria ($p = 0.0158$), Acidobacteria-6 ($p = 0.0070$), Spartobacteria ($p = 0.0351$), Gemmatimonadetes ($p = 0.0497$) and Planctomycetia ($p = 0.0375$) were more abundant in bulk soil than in the mesh bags (**Figure 1A**). For fungi, there were fewer Pezizomycetes ($p = 0.0397$) and more Dothideomycetes ($p = 0.0435$) inside the mesh bags than in the bulk soil samples (**Figure 1B**).

The differences by sample location (i.e., bulk soil vs. mesh bag) for all 16S and ITS operational taxonomic units (OTUs) were verified using Principal Component Analysis ($p = 0.001$ for 16S and 0.004 for ITS). The Simpson alpha diversity index of 16S OTUs showed higher diversity in mesh bags (0.994 ± 0.004) than in bulk soil (0.987 ± 0.007) after 6 months of incubation. On the other hand, the Simpson diversity index did not differ for the ITS

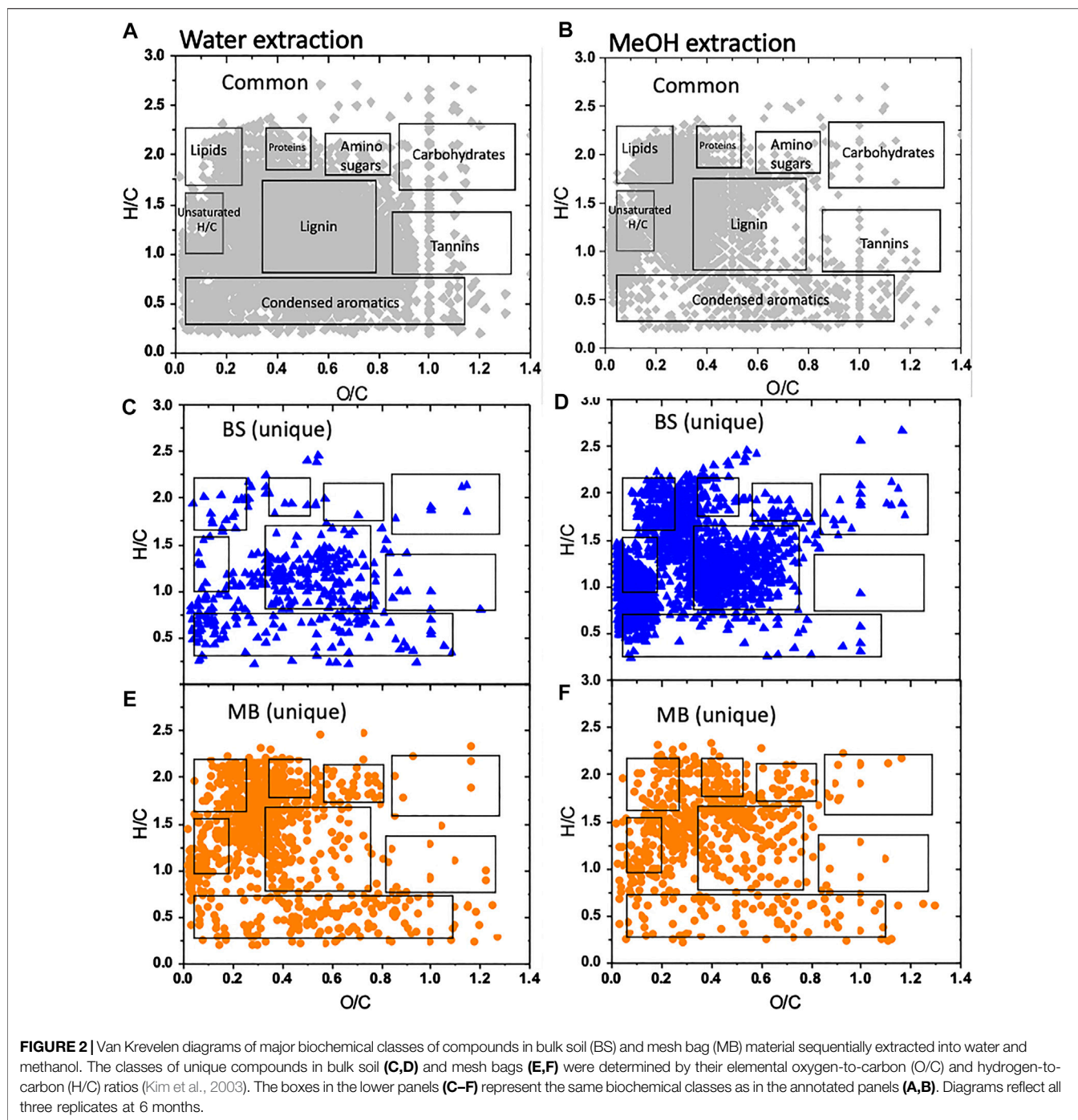


sequencing of mesh bag (0.85 ± 0.07) and bulk soil (0.86 ± 0.06) materials (**Supplementary Figures S1, S2**).

3.2 Fourier Transform Ion Cyclotron Resonance Mass Spectrometry Analysis of Water and Methanol Extracts of Organic Matter

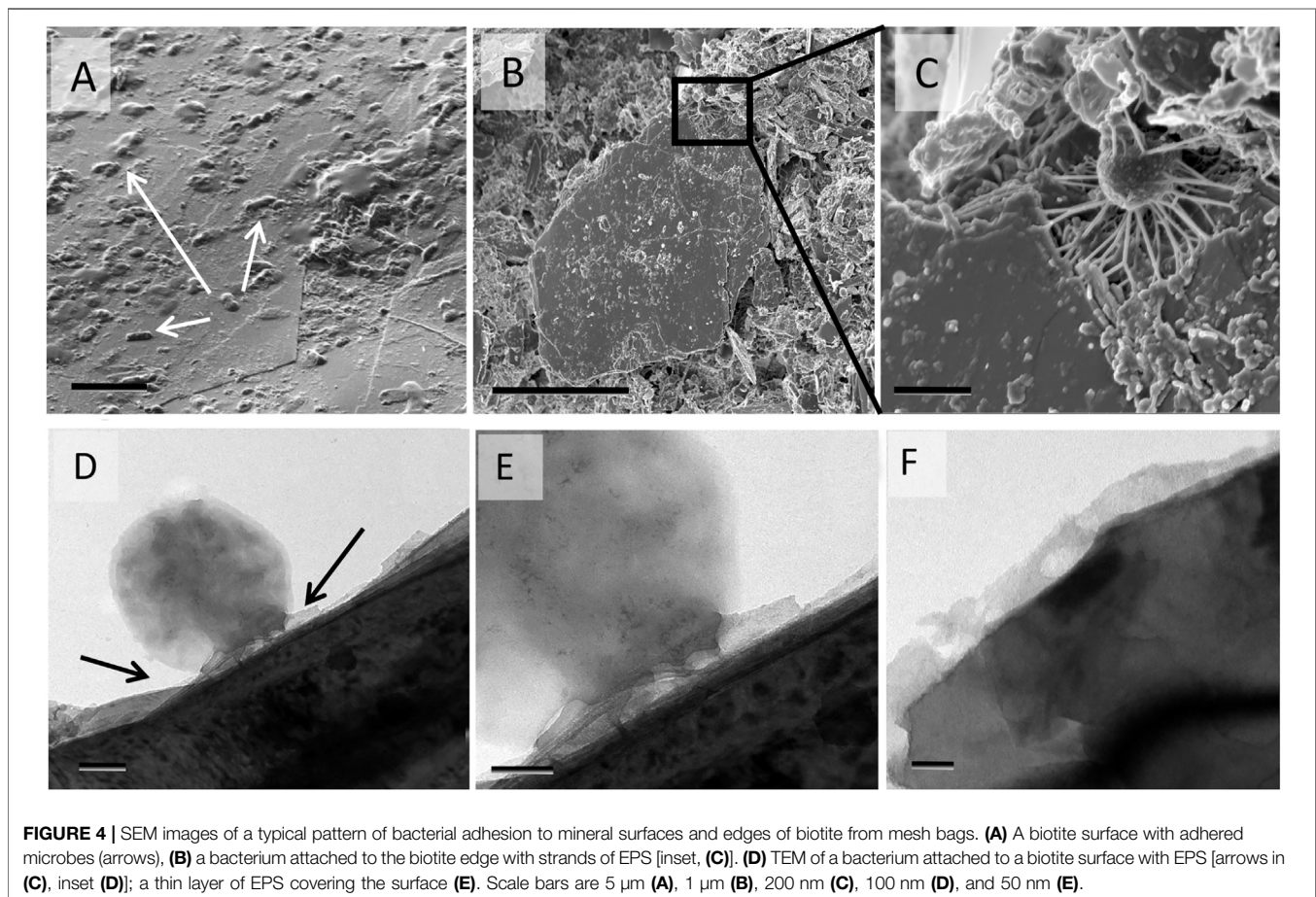
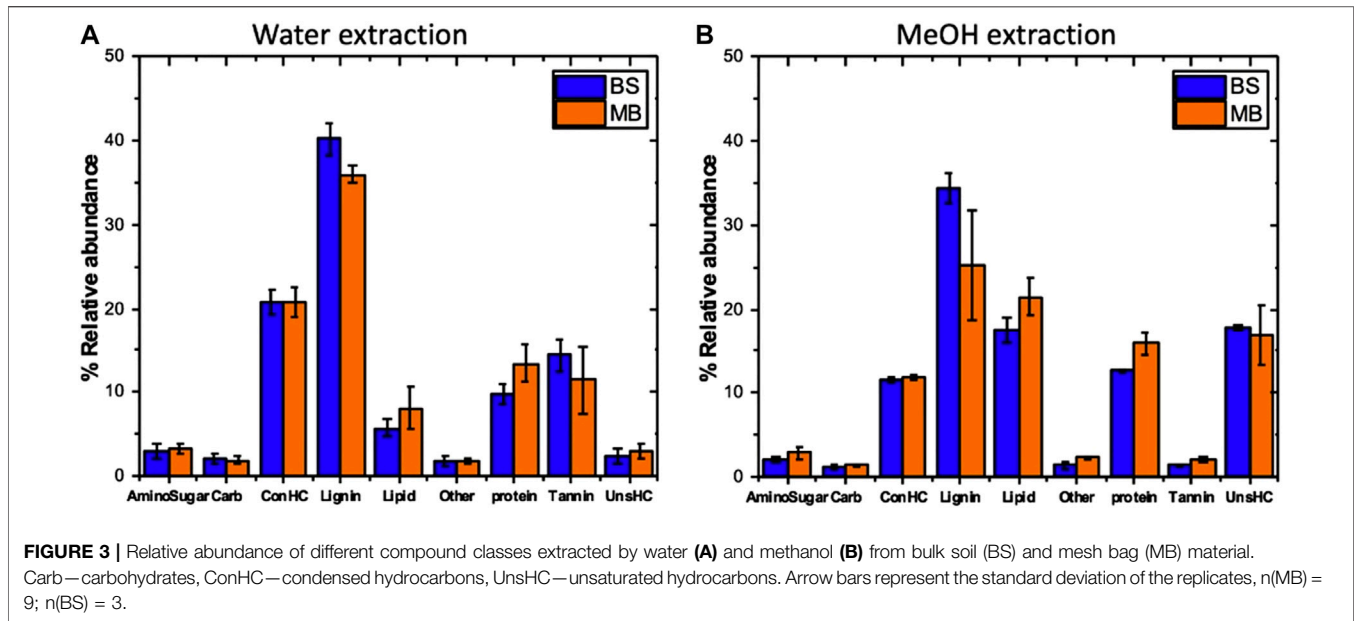
We characterized the molecular composition and complexity of the carbon compounds in the bulk soil and the newly formed associations with biotite in three mesh bags to address the hypothesis that the composition of the newly formed mineral-

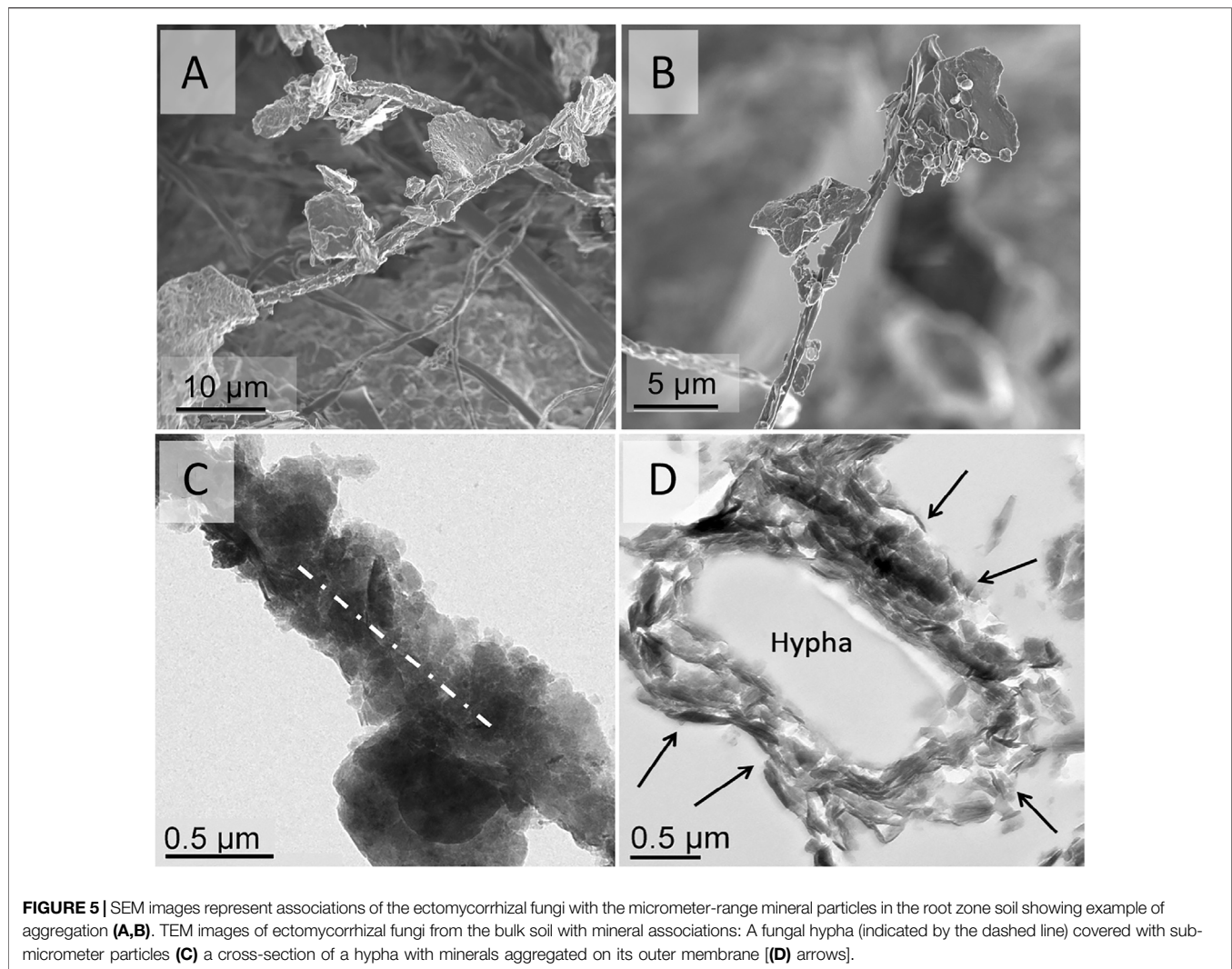
associated organic matter has a signature of microbial activity. The numbers of peaks observed in each solvent and for each sample type were relatively similar, but each solvent extracted a different class of compounds. The class of water extractable organic matter that could represent the most labile fraction of the SOM was around 60% unique to water extraction; 40% overlapped with the class of methanol extractable SOM in the mesh bags, while in bulk soil the overlap was only 22%. Compounds with low O/C ratios that fall in the lipid-like and unsaturated hydrocarbon regions of the van Krevelen diagram were more abundant in the mesh bag samples compared to the bulk soil, reflecting a microbial signature (Tfaily et al., 2017),



(Figures 2, 3). SOM in the bulk soil contained a higher abundance of lignin-like and CRAM (carboxylic-rich alicyclic molecules)-like compounds, reflecting plant signature. Additionally, protein-like material (mainly small peptides) was significantly more abundant in the mesh bags compared to bulk soil, further evidence of microbial signature in the bags and reflecting the high microbial activity taking place on biotite (Figure 3).

By nonmetric multidimensional scaling analysis (NMS), microbial community composition correlated well with the composition of organic matter measured by FTICR MS in samples collected at 6 months. Lipid-, protein- and unsaturated hydrocarbon-like compounds, and CHO compounds with P or S were associated with soil from inside the mesh bags, whereas CHON compounds (including CHONS, CHONP, and CHONSP) and amino sugar-, carbohydrate- and





condensed hydrocarbon-like compounds were associated with bulk soil.

3.3 Physicochemical Characteristics of Mesh Bags Content and Bulk Soil Particles

We used electron microscopic and x-ray spectrometric approaches to address our hypothesis that the SOM, microbial biopolymers, and adhered microbes and fungal hyphae cause physicochemical changes as a sign of biogenic mineral weathering.

Microbial biomass was adhered to biotite surfaces and edges, forming a thin amorphous layer of organic material that often enrobed the minerals. We observed the pattern of microbes colonizing the mineral edges and fractures for easier access to fresh surfaces with more accessible base cations (**Figure 4**).

The mesh bags also contained some bulk soil particles that were most likely transported through the 50 µm mesh by passive water flow. We assume no biota were involved in the

translocation of the bulk soil material. These minerals derived from the outer bulk soil, often in the <2 µm range, became readily aggregated into much larger units by the EPS that was formed by the microbes inside the bags (**Supplementary Figure S3**). In the bulk soil, root associated ectomycorrhizal fungal hyphae held small soil particles together that were five times larger in diameter than the fungal hyphae (**Figure 5**) and nanometer size particles were able to directly aggregate on the surface of the hyphae (**Figures 5C,D**).

SOM stabilization was observed in OM filled fractures (**Figures 6A,B**—arrows) and between layers (**Figures 6C,D**—arrows) of biotite in the mesh bag samples, providing physical protection of the organic matter from degradation.

Energy-dispersive X-ray spectrometry was used for elemental mapping of mineral surfaces to capture signs of base cation extraction by microbes and associated OM as one of the indicators of chemical weathering. As anticipated, the elemental concentrations were low (close to detection limits) in the organic matter, but Fe, Mg, and K was clearly detected in the MAOM (**Figure 7**).

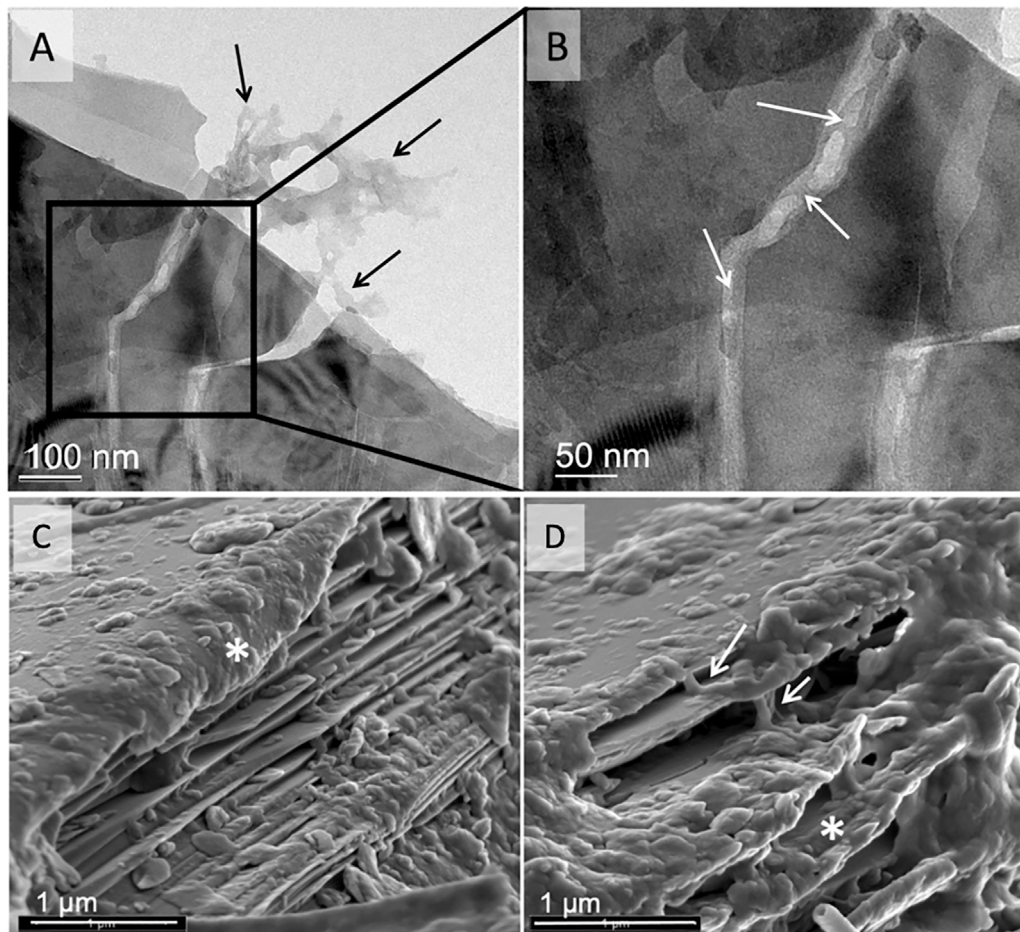


FIGURE 6 | TEM image of a biotite flake from the mesh bags, with organic matter adhered to its surfaces and edges [arrows in (A)], and filled into cracks [arrows in (B), inset of (A)]. Representative SEM images of mesh bag biotite edges covered with SOM. The expansion of the biotite layers allowed organic matter accumulation on the particle surface [asterisk in (C)] and between the layers [arrows in (D)].

Signs of physical weathering such as formation of cracks filled with organic materials (Figures 6A,B) and expansion of the original biotite layers (Figures 8B,C) covered with SOM (Figures 6C,D) were commonly observed on biotite from the mesh bags.

Additionally, sub-micron size mineral fractions were often immobilized and physically stabilized by the amorphous organic layer covering biotite particles (Figures 9A,B), forming organo-mineral assemblies (Figure 9C).

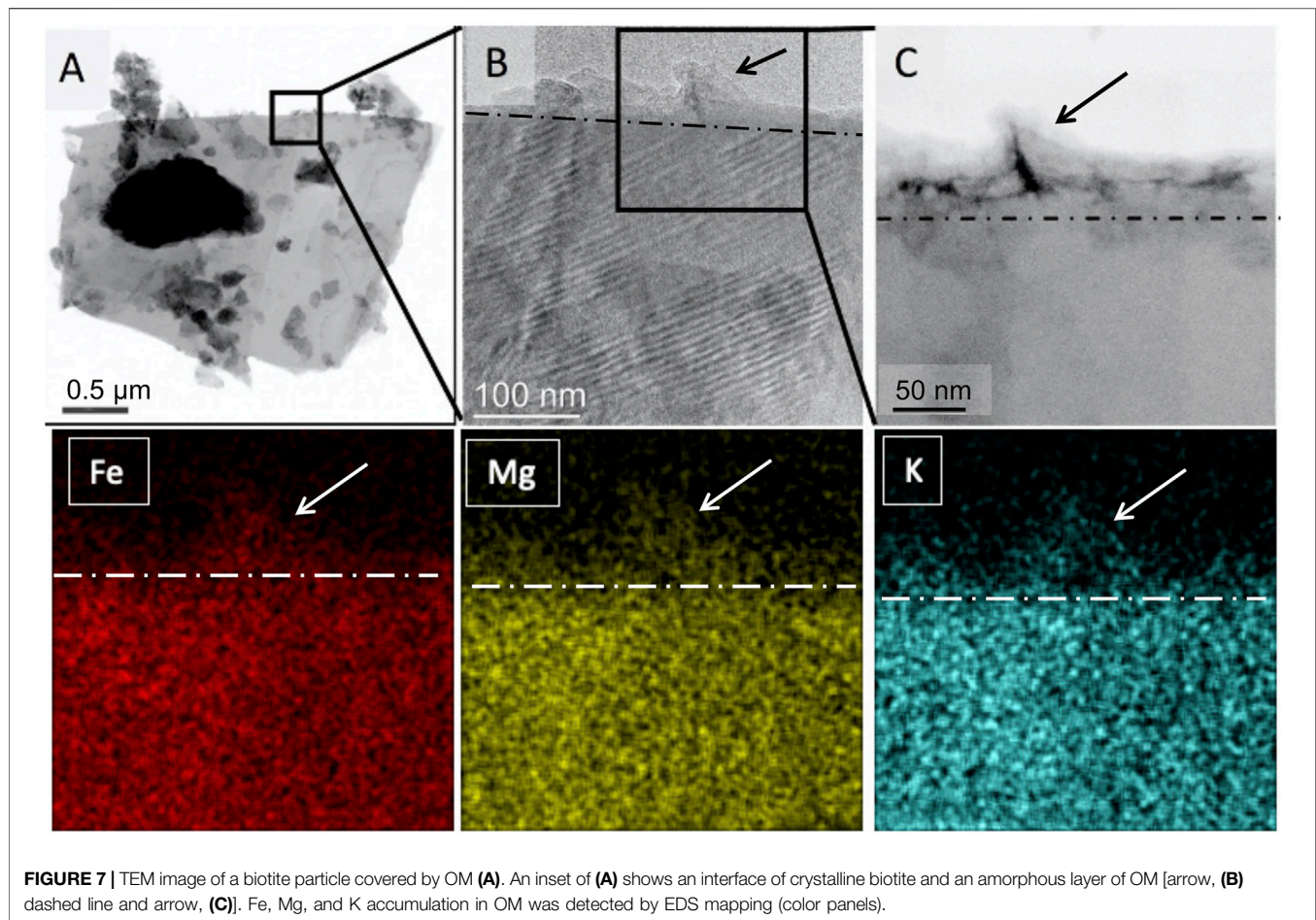
4 DISCUSSION

4.1 Microbiomes in Mesh Bags and Bulk Soil

Distinctly different bacterial and fungal communities were found in mesh bags compared to in the bulk soil after incubating pristine biotite particles in the root zone of *Ponderosa* pine for 6 months (Figure 1). Significant phylogenetic differences in alpha- and beta-diversity were observed among the mineral-associated bacteria as compared to the source microbiome in bulk soil

(Supplementary Figures S1, S2), with the bacterial microbiome differing more than the fungal.

The most abundant phyla associated with the particles in the mesh bags included Actinobacteria, Bacteroidetes and Proteobacteria (Figure 1A) which are among the most abundant bacterial groups in rhizosphere (Mendes et al., 2013) suggesting that we achieved our objective to locate the mesh bags in close proximity to the pine rhizosphere. Proteobacteria and Bacteroidetes have high affinity for mineral-microbe associations, especially if the mineral contains available iron (Ahmed et al., 2017). Biotite selected for our study contains a significant amount of divalent iron (Shi et al., 2014) that can easily be oxidized and released through bacterial and fungal weathering (Kelly et al., 2016; Bonneville et al., 2016). The greater abundance of Betaproteobacteria inside the mesh bags compared to the bulk soil (Figure 1A) specifically indicates microbially-mediated weathering of biotite in our study because Betaproteobacteria, especially in the genus *Burkholderia*, are known for high mineral-weathering capabilities that effectively mobilize iron (Lepleux et al., 2012; Kelly et al., 2016; Colin et al., 2017). In addition, the



decreased abundance of Acidobacteria and the increased abundance of Proteobacteria in mesh bags compared to bulk soil (Figure 1A) is in agreement with previously reported observations (Lepleux et al., 2012; Ahmed et al., 2017; Colin et al., 2017; Whitman et al., 2018) that the input of minerals into soils influences species abundance and creates microbial hotspots (Kuzayakov and Blagodatskaya, 2015). Uroz et al. (2015) introduced the concept of the mineralosphere, which states that minerals control the distribution and function of mineral-associated bacterial communities, and even though in our study we only compared one mineral to the bulk soil, the results are in agreement with findings of others (Hutchens et al., 2010; Uroz et al., 2015; Colin et al., 2017; Kleber et al., 2021). The higher abundance of bacteria with mineral-weathering capacity in mesh bags than in bulk soil (Figure 1A) supports the hypothesis that biotite promotes colonization by specifically adapted microbes that can preferentially release and use inorganic nutrients (Uroz et al., 2015). Also, similarly to grass land soils, the initial bacterial colonization of minerals (biotite) in the Ponderosa pine (dry forest) soils is selective based on the physicochemical characteristics of the minerals (Kandeler et al., 2019; Vieira et al., 2020; Boeddinghaus et al., 2021).

Ponderosa pine lives in association with ectomycorrhizal fungi and their root zone also contains saprophytic fungi, both of which

play a role in SOM decomposition (Phillips et al., 2014; Shah et al., 2016). The average fungal hypha diameter is 3–6 μm with a range of 1–30 μm (Bindschedler, et al., 2010); thus, it was expected that fungal hyphae would grow into the mesh bags (50 μm mesh size). Visual analyses of biotite surfaces mostly show bacteria and MAOM in the mesh bag (Figures 4, 6, 8), and small amount of fungal attachment (Supplementary Figure S4C). However, the ITS amplicon sequencing and subsequent taxonomic analysis revealed the presence of fungi in the mesh bags (Figure 1B). The composition of fungal taxa in the mesh bags was similar to that in the bulk soil, but the abundance of fungal taxa differed somewhat (Figure 1B). Agaricomycetes, a basidiomycote, remained at the highest abundance but lower than in the bulk soil, while the abundance (and proportion) of Dothideomycetes, the largest and most diverse class of Ascomycota (Schoch et al., 2009), significantly increased in mesh bags compared to in bulk soil (Figure 1B). Also, we found a presence of members of the Mucoraceae (div. Zygomycota), and Pezizomycetes in all samples (Figure 1B) that can be associated with *P. ponderosa* (Fujimura et al., 2005). It has been documented that symbiotic (mycorrhizal) fungi are the main colonizers of minerals (Colin et al., 2021 and references therein), which confirms the significant role of mycorrhizal fungi in nutrient cycling, tree nutrition and mineral

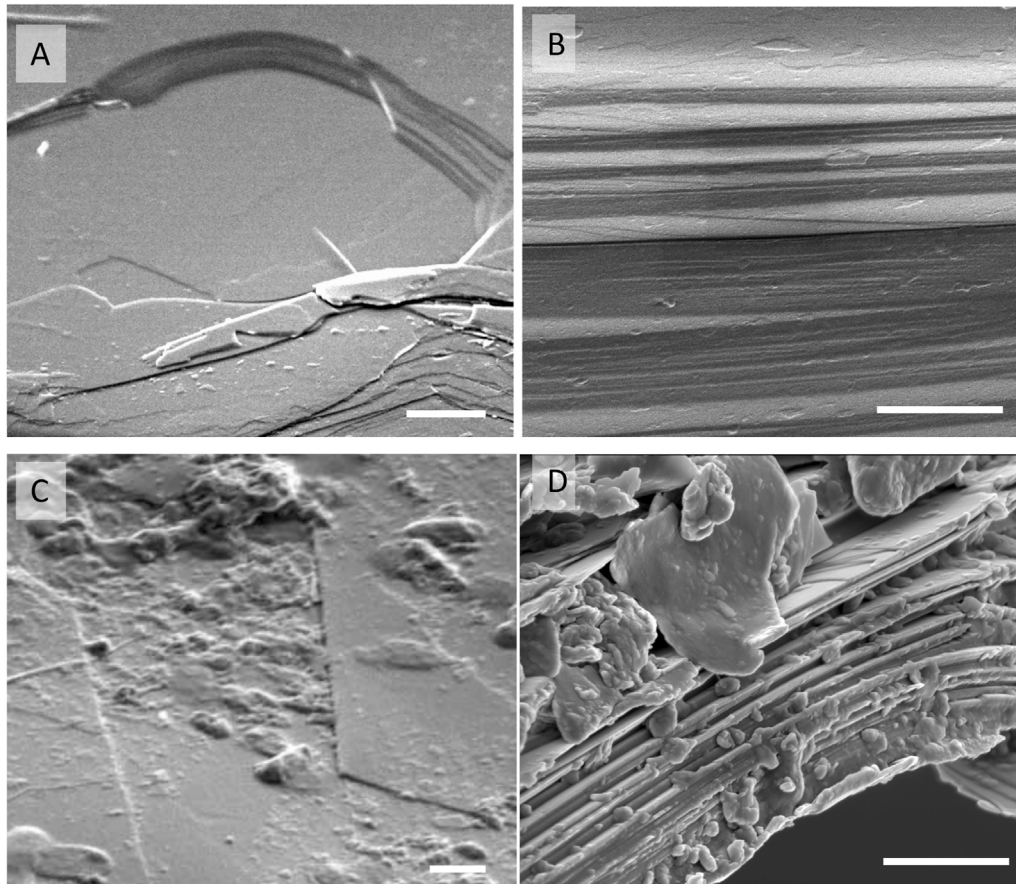


FIGURE 8 | Representative SEM images of control biotite planar surface **(A)** and edge **(B)** are unchanged after 6 months. Biotite incubated in soil are covered with adhered organic matter and bacteria on the planar surface **(C)** and OM fills between the biotite expanded layers **(D)** at the particle edges. Scale bars are 500 nm **(A,C)**, and 200 nm **(B,D)**.

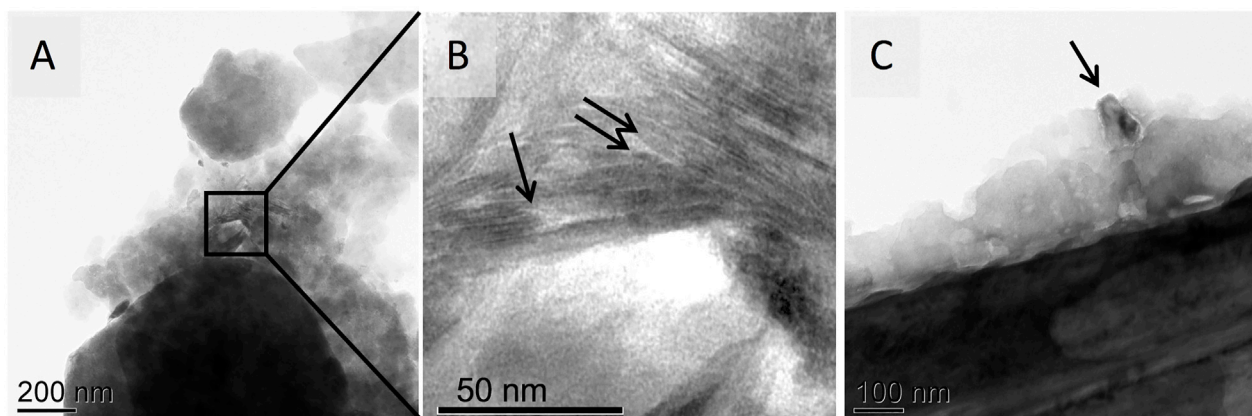


FIGURE 9 | TEM images of **(A)** a mesh bag biotite particle covered with amorphous organic layer that acted as a binding agent to immobilize sub-micron mineral fractions [inset in **(B)**]. A layered sheet structure (arrows) is characteristic of a phyllosilicate particle. **(C)** A 100-nm mineral fragment embedded in organic material, becoming a part of the SOM "shell" of encrusted immobilized nanoparticles.

weathering (Smits and Wallander, 2017). Without being able to analyze the genomes of the fungi we detected at the level of genera, we are not able to determine their importance in biotite colonization and weathering. However, known fungal growth strategies indicate that fungal hyphae reach new mineral surfaces first (Kandeler et al., 2019) and then the “fungal highways” help the mobilization of bacteria into the mesh bags (Simon et al., 2017; Whitman et al., 2018; Sun et al., 2020). Colin et al. (2021) argue that while mineral type affects fungal colonization, the land cover plants are the main drivers of the fungal community structure, which is consistent with our results of finding taxa in the mesh bags that are commonly associated with *Ponderosa* pine.

4.2 Molecular Composition of Organic Matter in Mesh Bags and Bulk Soil

High resolution FTICR mass spectrometry provided clear evidence of the microbial signature inside the mesh bags and, in contrast, a higher content of plant signatures was observed in the bulk soil (Figure 2). These results support the hypothesis that the biotite-associated organic matter in the mesh bags has a signature of microbial activity. The VK diagrams show that the extracts from the mesh bag biotite were enriched in protein-(peptides) and lipid-like compounds (Figures 2E,F)—signatures of microbial activity (Tfaily et al., 2014), whereas extracts from the bulk soil included higher amount of lignin-like compounds that are plant signatures (Figures 2C,D). Microbial decomposition of plant-derived substrates constitute the first step in formation of MAOM (Raczka et al., 2021) which is one of the mechanisms of SOM formation; the other is formation of aggregates (Angst et al., 2021). The rate and proportion of microbial decomposition and formation of MAOM depends on interactions between microbial diversity and substrate chemistry (Raczka et al., 2021). A recent review (Angst et al., 2021) discusses the idea that plant biomolecules might account for about half of the stabilized SOM in aggregates and MAOM, while the other half is comprised of microbial compounds; however, there is still a large uncertainty. Our results show that the majority of the newly formed OM in the mesh bags is microbial biomass and the product of microbial transformation (Figures 4, 6), while other organic residues were washed into the mesh bags (Supplementary Figures S4A,B), as shown by high abundance of lignin-like compounds (Figure 3). The enhanced production of lipid-like and protein like compounds (Figures 2E,F) due to the localized microbial activity as seen in the mesh bags (Figure 4) can represent a variety of interconnected processes ongoing in the rhizosphere of the pine where microbial activity is higher than in the bulk soil (Kleber et al., 2015; Qafoku, 2015). Relative abundances of lipids and proteins were higher in the mesh bags than in the bulk soil in both the water and methanol extracts (Figure 3). These compound drive organic carbon stabilization (Spaccini et al., 2002; von Lutzow et al., 2006; Song et al., 2013) by facilitating adsorption to mineral surfaces (Figures 4D–F), aggregation (Figure 5), and creating a micro-environment of physical and chemical inaccessibility (Figures 6D,E; Kleber et al., 2021).

However, the higher proportion of proteins in mesh bags could also indicate the accumulation of microbial cell-envelope fragments (Schurig et al., 2012) and necromass (Liang et al., 2019; Käßner et al., 2021) that are also of microbial origin and can contribute to MAOM (Creamer et al., 2019).

4.3 Characteristics of the Mineral-Associated Organic Matter and Weathering of Mineral Surfaces

The organic compounds found in the mesh bags were associated with biotite, either by directly adhering to its planar or edge surfaces, or causing microaggregation of smaller particles and promoting organic carbon stabilization. Adsorption was observed as bacterial cells and their EPS covered the planar surfaces (Figures 4A,D,E) and anchored themselves into broken corners of the mineral particles (Figures 4B,C). Prominent layers of organic matter covered the mineral edges and filled the gaps between layers (Figures 6C,D). As the mesh bag content had similar texture as the surrounding bulk soil, water could easily flow through and most likely carried dissolved organic matter and small particles (<50 μm) that contributed to MAOM formation, which is supported by the composition of the mesh bag extracts (Figures 2, 3) and visual accumulation of “washed in” materials (Supplementary Figures S4A,B). These reactive coatings on the mineral surfaces had a great potential to control the ionic exchange between solids and fluids, with water acting as a conduit. Biotite is a 2:1 phyllosilicate with permanent negative charges if the tetrahedral layer has cation substitutions that allow electrostatic attraction of metal cations (Sposito et al., 1999). However, if there is no significant substitution and the surface remain neutral, organic matter can accumulate by hydrophobic exclusion (Willemssen et al., 2019). Also, the hydroxyl groups can be exposed and protonate at the biotite edges, and ligand exchange can occur (Bray et al., 2015) that retains organic matter (Kleber et al., 2021). Visualization by SEM show that the edges were thickly covered in OM that also entered the space between the expanded cleavage planes (Figures 6C,D). These intercalations between the biotite layers caused visible alteration to the biotite structure. We assume the intercalation we observed might be due to easier spatial accessibility for microbial decomposition rather than to chemical lability, in accordance with the soil continuum model presented by (Lehmann and Kleber, 2015). Their concept emphasizes the importance of spatial inaccessibility, such as in microaggregates or pores, rather than SOM being merely “stable in nature” with regard to mineral protection of OM. The spatial inaccessibility can provide a physical protection from further dissociation and from microbial attacks (von Lutzow et al., 2006; Kaiser and Guggenberger, 2007; Lehmann and Kleber, 2015). The physical stabilization of organic matter also occurred in micro- and nano-cracks and pores of the particles (Figures 6A,B) which can provide physical isolation and protect MOAM from degradation and decomposition (Kleber et al., 2015). Microaggregation that can serve as physical stabilization was detected on hyphal conduits just outside the mesh bags (Figures 5A,B) and fungal hyphae were encrusted in sub-micrometer or

nanometer size particles (**Figures 5C,D**). Microaggregation was also found and visualized by TEM in the mesh bags, where bulk soil particles (Ca-Na feldspars) were confirmed by EDS in the assembly (**Supplementary Figure S3**). These organo-mineral microaggregates are considered structural units and building blocks for soil aggregation, microhabitats, and stabilization places for lignin and lipids (Angst et al., 2017; Totsche et al., 2018). The MAOM layer also is able to isolate and physically trap and stabilize submicron to nanometer-scale mineral fragments (**Figure 9**) that most likely alter chemically over time. These mineral fragments are bound by a variety of bonds and forces, mostly based on their chemical composition, charge and size, and incorporated into the continuously changing MAOM, (Kogel-Knabner et al., 2008; Kleber et al., 2015).

Chemical stabilization of organic matter on mineral surfaces and weathering are directly connected. Newly released cations such as Fe, Mg, and K were absorbed in MAOM (**Figure 7**), which supports the idea that microbial cation extraction during biotite weathering is executed *via* local acidification, targeted excretion of ligands, and mobilization of Fe, Al, Mg and K (Bonneville et al., 2016). The extracted cations can undergo further reactions such as cation exchange and covalent bonding, or contribute to other processes such as dissolution, precipitation, transformation of minerals and metals, redox and/or complexation reactions involved in weathering and MAOM stabilization. Our previous studies (Balogh-Brunstad et al., 2008; 2017) and other published studies (Taylor et al., 2009) indicate that biofilms, EPS, and any organic layers on soil mineral surfaces have an important regulatory role in simultaneously increasing chemical weathering and decreasing chemical loss of elements. We also found that microbial EPS and biofilm in the rhizosphere of pine have great adsorptive capacity and enhance mineral weathering (Fredrickson and Fletcher, 2001; Dohnalkova et al., 2011). Our coupled TEM and EDS analysis show the accumulation of key elements (K, Fe, and Mg) in the MAOM that most likely originated from the biotite as the pixel densities of the EDS maps decreased from the biotite toward the edge of the organic cover (**Figure 7**). Also, significant changes of roughness and widened spacing of the layers were observed on the biotite particles in addition to bacteria and organic matter adsorption, both on the planar surfaces and the edges, compared to on the original and control mineral particles (**Figure 8**). These observations support the hypothesis that MAOM cause physicochemical changes to the biotite as a sign of biogenic mineral weathering. While our field experiment did not have a true abiotic control (a mesh bag that exclude microbes with <0.1 μm openings), we expected that MAOM and associated microbial activity would increase and localize biotite alteration compared to under abiotic conditions (Bonneville et al., 2011, Bonneville et al., 2016; Balogh-Brunstad et al., 2017). The buried mesh bags were simultaneously exposed to abiotic and biotic weathering forces that could not be separated in our study and we did not aim to quantify weathering rates in the mesh bags, but to document the MAOM and biotite alteration as sign of biogenic weathering. The column growth experiments previously conducted by our research group found clear evidence that ectomycorrhizal fungi and associated bacteria stimulated biotite weathering compared to in abiotic controls (Shi et al., 2014;

Balogh-Brunstad et al., 2017). Also, the presence of organic ligands, even at low concentrations, increased the release of di- and tri-valent metals from biotite compared the inorganic acid (acidification) alone without significant increase of biotite weathering rates (Bray et al., 2015). Based on experimental evidence abiotic weathering should dominate, especially, under wet conditions (such as the wet season of our study), but weathering under organic (biofilm) cover could be important on an ecosystem scale because elemental losses would be reduced (Balogh-Brunstad et al., 2008). The level of hydration plays a critical role in MAOM stabilization as seasonal dehydration can increase its ionic strength and induce physical contraction, collapse, and reorganization of macromolecular structures or the reverse processes that can occur when water is present (Lawrence et al., 2009).

Many signs of abiotic and biotic biotite weathering are indistinguishable. These include the instability of interlayers, allowing cation exchange to alter interlayer cation composition (Bonneville et al., 2016; Bower et al., 2016) and the formation of secondary mineral weathering products such as transition to vermiculite and smectite clays, or neof ormation of kaolin-group minerals and gibbsite (Price and Velbel, 2014). Arocena et al. (2012) point out that the transformation of biotite and K-uptake also depends on the plant-fungus symbiotic system, and the formation of clay minerals will then be a function of plant type and symbiotic relations in the soils. We expected to see alteration of the crystal structure, formation of secondary mineral phases and the increase of amorphous content in the mesh bags biotite as the sign of weathering, which may have been enhanced by the MAOM accumulation. We could not confirm and quantify these expectations. Nonetheless, the XRD results indicated subtle mineral transformation (**Supplementary Figure S6**), and a slight decrease in crystallite size, and a slight increase in amorphous content (**Supplementary Figure S7**). However, due to the low number of replicates (4) and the limitations of separating potentially infiltrated bulk soil particles from the *in-situ* formed secondary materials in the mesh bag, we interpret these results cautiously (**Supplementary Material**).

5 CONCLUSION

The microbial origin of MAOM previously was documented on biotite surfaces in laboratory experiments (e.g., Dohnalkova et al., 2017; Angst et al., 2021) and we were able to show the presence of microbially produced newly formed organic matter (particularly protein/peptide and lipid-like compounds) in mesh bags in a field experiment (**Figures 2, 3**). Also, MAOM was adsorbed to biotite surfaces (**Figures 4, 6, 8**) and formed microaggregates (**Figure 7, Supplementary Figure S3**) that altered the biotite by elemental uptake (**Figure 7**) and physical distortion of the layers (**Figures 6, 8**). The results provide supporting evidence for our hypotheses, while we were unable to separate abiotic and biotic signatures of weathering, and thus were unable to quantify the alteration of biotite by the applied methods. However, this study showed the direct and indirect involvement of soil microbial communities in the formation of MAOM, soil organic carbon stabilization,

microaggregation, and mineral weathering and micro- and nano-scales. Applying the mesh bag technique in combination of molecular and micro- and nano-scale analytical techniques to study MAOM on soil minerals is promising and provides an opportunity to understand MAOM formation under natural soil conditions. Further studies are encouraged with larger replication of a wider variety of minerals, soil types, and climate conditions.

DATA AVAILABILITY STATEMENT

The datasets presented in this study can be found in online repositories. The names of the repository/repositories and accession number(s) can be found below: BioProject, accession number PRJNA827521.

AUTHOR CONTRIBUTIONS

AD designed the experiment and the analytical approach, performed the EM imaging and wrote the paper; MT and RC designed the FTICR analytical approach, performed the FTICR experiment, data analysis and co-wrote the paper; AS provided correlative DNA and FTICR data analyses and co-wrote the paper, CB performed bioinformatics analyses and DNA data visualization; TV performed XRD, analyzed data and co-wrote the paper; AC acquired material for 16S rRNA sequencing; LK performed HR-S/TEM imaging and elemental mapping; and LT, JH, and CK all co-created and thoroughly reviewed the paper, and contributed to the revisions. ZB-B directed the manuscript writing effort and co-wrote the revisions.

REFERENCES

- Acker, J. G., and Bricker, O. P. (1992). The Influence of pH on Biotite Dissolution and Alteration Kinetics at Low Temperature. *Geochimica Cosmochimica Acta* 56, 3073–3092. doi:10.1016/0016-7037(92)90290-y
- Ahmed, E., Hugerth, L. W., Logue, J. B., Brüchert, V., Andersson, A. F., and Holmström, S. J. M. (2017). Mineral Type Structures Soil Microbial Communities. *Geomicrobiol. J.* 34, 538–545. doi:10.1080/01490451.2016.1225868
- Angst, G., Mueller, K.E., Kögel-Knabner, I., Freeman, K.H., and Mueller, C.W. (2017). Aggregation controls the stability of lignin and lipids in clay-sized particulate and mineral associated organic matter. *Biogeochemistry* 132, 307–324.
- Angst, G., Mueller, K. E., Nierop, K. G. J., and Simpson, M. J. (2021). Plant- or Microbial-Derived? A Review on the Molecular Composition of Stabilized Soil Organic Matter. *Soil Biol. Biochem.* 156. doi:10.1016/j.soilbio.2021.108189
- Arocena, J. M., Velde, B., and Robertson, S. J. (2012). Weathering of Biotite in the Presence of Arbuscular Mycorrhizae in Selected Agricultural Crops. *Appl. Clay Sci.* 64, 12–17. doi:10.1016/j.clay.2011.06.013
- Aronesty, E. (2011). Command-line tools for processing biological sequencing data. Available at: <https://github.com/ExpressionAnalysis/ea-utils>.
- Balogh-Brunstad, Z., Keller, C., Shi, Z., Wallander, H., and Stipp, S. (2017). Ectomycorrhizal Fungi and Mineral Interactions in the Rhizosphere of Scots and Red Pine Seedlings. *Soils* 1, 5. doi:10.3390/soils1010005
- Balogh-Brunstad, Z., Kent Keller, C., Thomas Dickinson, J., Stevens, F., Li, C. Y., and Bormann, B. T. (2008). Biotite Weathering and Nutrient Uptake by Ectomycorrhizal Fungus, *Suillus Tomentosus*, in Liquid-Culture

FUNDING

Financial support was provided by PNNL's Laboratory Directed Research and Development (LDRD) program and NSF grant EAR 09-52399.

ACKNOWLEDGMENTS

This research was performed at the Environmental Molecular Sciences Laboratory (EMSL), a national scientific user facility sponsored by the Department of Energy's Office of Biological and Environmental Research, located at the Pacific Northwest National Laboratory. PNNL is operated for DOE by Battelle Memorial Institute under Contract# DE-AC05-76RL0-1830. We gratefully acknowledge Sarah Owens' group at the Biosciences Division's Environmental Sample Preparation and Sequencing Core at Argonne National Laboratory for the sequencing work. AD thanks Daniel Dohnalek and Hugo Bodik for assistance during the field sampling. AD also thanks Odeta Qafoku for her help with EDS analysis of fungal-mineral associations. Finally, we sincerely thank the journal peer reviewers for their expert, constructive comments and insightful suggestions.

SUPPLEMENTARY MATERIAL

The Supplementary Material for this article can be found online at: <https://www.frontiersin.org/articles/10.3389/feart.2022.799694/full#supplementary-material>

- Experiments. *Geochimica Cosmochimica Acta* 72, 2601–2618. doi:10.1016/j.gca.2008.04.003
- Banfield, J. F. N. K. H. M. S. O. A. S. C. O. G. (1997). *Geomicrobiology: Interactions between Microbes and Minerals*. Washington, D.C. Mineralogical Society of America.
- Bindschedler, S., Millièrè, L., Cailleau, G., Job, D., and Verrecchia, E.P. (2010). Calcitic nanofibres in soils and caves: a putative fungal contribution to carbonatogenesis. *Geological Society, London, Special Publications* 336, 225.
- Boeddinghaus, R.S., Marhan, S., Gebala, A., Haslwimmer, H., Vieira, S., Sikorski, J., et al. (2021). The mineralosphere—interactive zone of microbial colonization and carbon use in grassland soils. *Biology and Fertility of Soils* 57, 587–601.
- Bonneville, S.C., Morgan, D., Schmalenberger, A., Bray, A., Banwart, S., and Benning, L. (2011). Tree-mycorrhiza symbiosis accelerate mineral weathering: Evidences from nanometer-scale elemental fluxes at the hypha-mineral interface. *Geochimica et Cosmochimica Acta* 22, 6988–7005.
- Bonneville, S., Bray, A. W., and Benning, L. G. (2016). Structural Fe(II) Oxidation in Biotite by an Ectomycorrhizal Fungi Drives Mechanical Forcing. *Environ. Sci. Technol.* 50, 5589–5596. doi:10.1021/acs.est.5b06178
- Bower, W. R., Pearce, C. I., Smith, A. D., Pimblott, S. M., Mosselmans, J. F. W., Haigh, S. J., et al. (2016). Radiation Damage in Biotite Mica by Accelerated α -particles: A Synchrotron Microfocus X-Ray Diffraction and X-Ray Absorption Spectroscopy Study. *Am. Mineralogist* 101, 928–942. doi:10.2138/am-2016-5280ccbyncnd
- Bray, A. W., Benning, L. G., Bonneville, S., and Oelkers, E. H. (2014). Biotite Surface Chemistry as a Function of Aqueous Fluid Composition. *Geochimica Cosmochimica Acta* 128, 58–70. doi:10.1016/j.gca.2013.12.002
- Bray, A. W., Oelkers, E. H., Bonneville, S., Wolff-Boenisch, D., Potts, N. J., Fones, G., et al. (2015). The Effect of pH, Grain Size, and Organic Ligands on Biotite

- Weathering Rates. *Geochimica Cosmochimica Acta* 164, 127–145. doi:10.1016/j.gca.2015.04.048
- Caporaso, J. G., Kuczynski, J., Stombaugh, J., Bittinger, K., Bushman, F. D., Costello, E. K., et al. (2010). QIIME Allows Analysis of High-Throughput Community Sequencing Data. *Nat. Methods* 7, 335–336. doi:10.1038/nmeth.f.303
- Caporaso, J. G., Lauber, C. L., Walters, W. A., Berg-Lyons, D., Huntley, J., Fierer, N., et al. (2012). Ultra-high-throughput Microbial Community Analysis on the Illumina HiSeq and MiSeq Platforms. *ISME J.* 6, 1621–1624. doi:10.1038/ismej.2012.8
- Chen, C., Dynes, J. J., Wang, J., Karunakaran, C., and Sparks, D. L. (2014). Soft X-Ray Spectromicroscopy Study of Mineral-Organic Matter Associations in Pasture Soil Clay Fractions. *Environ. Sci. Technol.* 48, 6678–6686. doi:10.1021/es405485a
- Chenu, C., and Plante, A. F. (2006). Clay-sized Organo-Mineral Complexes in a Cultivation Chronosequence: Revisiting the Concept of the 'primary Organo-Mineral Complex'. *Eur. J. Soil Sci.* 57, 596–607. doi:10.1111/j.1365-2389.2006.00834.x
- Colin, Y., Nicolitch, O., Turpault, M. P., and Uroz, S. (2017). Mineral Types and Tree Species Determine the Functional and Taxonomic Structures of Forest Soil Bacterial Communities. *Appl. Environ. Microbiol.* 83. doi:10.1128/AEM.02684-16
- Colin, Y., Turpault, M.-P., Fauchery, L., Buée, M., and Uroz, S. (2021). Forest Plant Cover and Mineral Type Determine the Diversity and Composition of Mineral-Colonizing Fungal Communities. *Eur. J. Soil Biol.* 105, 103334. doi:10.1016/j.ejsobi.2021.103334
- Courty, P.-E., Buée, M., Diedhiou, A. G., Frey-Klett, P., Le Tacon, F., Rineau, F., et al. (2010). The Role of Ectomycorrhizal Communities in Forest Ecosystem Processes: New Perspectives and Emerging Concepts. *Soil Biol. Biochem.* 42, 679–698. doi:10.1016/j.soilbio.2009.12.006
- Cremer, C.A., Foster, A.L., Lawrence, C., Mcfarland, J., Schulz, M., and Waldrop, M.P. (2019). Mineralogy dictates the initial mechanism of microbial necromass association. *Geochimica et Cosmochimica Acta* 260, 161–176.
- Dohnalkova, A. C., Marshall, M. J., Arey, B. W., Williams, K. H., Buck, E. C., and Fredrickson, J. K. (2011). Imaging Hydrated Microbial Extracellular Polymers: Comparative Analysis by Electron Microscopy. *Appl. Environ. Microbiol.* 77, 1254–1262. doi:10.1128/aem.02001-10
- Dohnalkova, A., Tfaily, M., Smith, A., Chu, R., Crump, A., Brislawn, C., et al. (2017). Molecular and Microscopic Insights into the Formation of Soil Organic Matter in a Red Pine Rhizosphere. *Soils* 1, 4. doi:10.3390/soils1010004
- Dontsova, K., Balogh-Brunstad, Z., and Chorover, J. (2020). Plants as Drivers of Rock Weathering. *Biogeochem. Cycles* 2020, 33–58. doi:10.1002/9781119413332.ch2
- Edgar, R. C., Haas, B. J., Clemente, J. C., Quince, C., and Knight, R. (2011). UCHIME Improves Sensitivity and Speed of Chimera Detection. *Bioinformatics* 27, 2194–2200. doi:10.1093/bioinformatics/btr381
- Finlay, R. D., Mahmood, S., Rosenstock, N., Bolou-Bi, E. B., Köhler, S. J., Fahad, Z., et al. (2020). Reviews and Syntheses: Biological Weathering and its Consequences at Different Spatial Levels - from Nanoscale to Global Scale. *Biogeosciences* 17, 1507–1533. doi:10.5194/bg-17-1507-2020
- Fredrickson, J. K., and Fletcher, M.A. (2001). *Subsurface Microbiology and Biogeochemistry*. Hoboken, NJ, USA: Wiley-Liss.
- Fujimura, K.E., Smith, J.E., Horton, T.R., Weber, N.S., and Spatafora, J.W. (2005). Pezizalean mycorrhizas and sporocarps in ponderosa pine (*Pinus ponderosa*) after prescribed fires in eastern Oregon, USA. *Mycorrhiza* 15, 79–86.
- Gorby, Y. A., Yanina, S. V., Moyles, D., Mclean, J. S., Rosso, K. M., Beveridge, T. J., et al. (2006). NUCL 74-Bacterial Nanowires: Electrically Conductive, Redox-Reactive Appendages Produced by Dissimilatory Metal Reducing Bacteria. *Abstr. Pap. Am. Chem. Soc.* 232.
- Hutchens, E., Gleeson, D., McDermott, F., Miranda-Casoluengo, R., and Clipson, N. (2010). Meter-Scale Diversity of Microbial Communities on a Weathered Pegmatite Granite Outcrop in the Wicklow Mountains, Ireland; Evidence for Mineral Induced Selection? *Geomicrobiol. J.* 27, 1–14. doi:10.1080/01490450903232157
- Hutchens, E. (2009). Microbial Selectivity on Mineral Surfaces: Possible Implications for Weathering Processes. *Fungal Biol. Rev.* 23, 115–121. doi:10.1016/j.fbr.2009.10.002
- Jackson, O., Quilliam, R. S., Stott, A., Grant, H., and Subke, J.-A. (2019). Rhizosphere Carbon Supply Accelerates Soil Organic Matter Decomposition in the Presence of Fresh Organic Substrates. *Plant Soil* 440, 473–490. doi:10.1007/s11104-019-04072-3
- Janusz, G., Pawlik, A., Sulej, J., Świdarska-Burek, U., Jarosz-Wilkolazka, A., and Paszczyński, A. (2017). Lignin Degradation: Microorganisms, Enzymes Involved, Genomes Analysis and Evolution. *Fems Microbiol. Rev.* 41, 941–962. doi:10.1093/femsre/fux049
- Janzen, H. H. (2006). The Soil Carbon Dilemma: Shall We Hoard it or Use it? *Soil Biol. Biochem.* 38, 419–424. doi:10.1016/j.soilbio.2005.10.008
- Jastrow, J. D., Miller, R. M., and Lussenhop, J. (1998). Contributions of Interacting Biological Mechanisms to Soil Aggregate Stabilization in Restored prairie! The Submitted Manuscript Has Been Created by the University of Chicago as Operator of Argonne National Laboratory under Contract No. W-31-109-ENG-38 with the U.S. Department of Energy.1. *Soil Biol. Biochem.* 30, 905–916. doi:10.1016/s0038-0717(97)00207-1
- Kaiser, K., and Guggenberger, G. (2007). Sorptive Stabilization of Organic Matter by Microporous Goethite: Sorption into Small Pores vs. Surface Complexation. *Eur J Soil Sci.* 58, 45–59. doi:10.1111/j.1365-2389.2006.00799.x
- Kalinowski, B. E., and Schweda, P. (1996). Kinetics of Muscovite, Phlogopite, and Biotite Dissolution and Alteration at pH 1?4, Room Temperature. *Geochimica Cosmochimica Acta* 60, 367–385. doi:10.1016/0016-7037(95)00411-4
- Kandeler, E., Gebala, A., Boeddinghaus, R. S., Müller, K., Rennert, T., Soares, M., et al. (2019). The Mineralosphere - Succession and Physiology of Bacteria and Fungi Colonising Pristine Minerals in Grassland Soils under Different Land-Use Intensities. *Soil Biol. Biochem.* 136, 107534. doi:10.1016/j.soilbio.2019.107534
- Kästner, M., Miltner, A., Thiele-Bruhn, S., and Liang, C. (2021). Microbial Necromass in Soils—Linking Microbes to Soil Processes and Carbon Turnover. *Frontiers in Environmental Science* 9.
- Keiluweit, M., Bougoure, J. J., Zeglin, L. H., Myrold, D. D., Weber, P. K., Pett-Ridge, J., et al. (2012). Nano-scale Investigation of the Association of Microbial Nitrogen Residues with Iron (Hydr)oxides in a Forest Soil O-Horizon. *Geochimica Cosmochimica Acta* 95, 213–226. doi:10.1016/j.gca.2012.07.001
- Kelly, L. C., Colin, Y., Turpault, M.-P., and Uroz, S. (2016). Mineral Type and Solution Chemistry Affect the Structure and Composition of Actively Growing Bacterial Communities as Revealed by Bromodeoxyuridine Immunocapture and 16S rRNA Pyrosequencing. *Microb. Ecol.* 72, 428–442. doi:10.1007/s00248-016-0774-0
- Kim, S., Kramer, R. W., and Hatcher, P. G. (2003). Graphical Method for Analysis of Ultrahigh-Resolution Broadband Mass Spectra of Natural Organic Matter, the Van Krevelen Diagram. *Anal. Chem.* 75, 5336–5344. doi:10.1021/ac034415p
- Kleber, M., Bourg, I. C., Coward, E. K., Hansel, C. M., Myneni, S. C. B., and Nunan, N. (2021). Dynamic Interactions at the Mineral-Organic Matter Interface. *Nat. Rev. Earth Environ.* 2, 402–421. doi:10.1038/s43017-021-00162-y
- Kleber, M., Eusterhues, K., Keiluweit, M., Mikutta, C., Mikutta, R., and Nico, P. S. (2015). Mineral-organic Associations: Formation, Properties, and Relevance in Soil Environments. *Adv. Agron.* 130, 1–140. doi:10.1016/bs.agron.2014.10.005
- Kogel-Knabner, I., Guggenberger, G., Kleber, M., Kandeler, E., Kalbitz, K., Scheu, S., et al. (2008). Organo-mineral Associations in Temperate Soils: Integrating Biology, Mineralogy, and Organic Matter Chemistry. *J. Plant Nutr. Soil Sci.* 171, 61–82.
- Kopittke, P. M., Dalal, R. C., Hoeschen, C., Li, C., Menzies, N. W., and Mueller, C. W. (2020). Soil Organic Matter Is Stabilized by Organo-Mineral Associations through Two Key Processes: The Role of the Carbon to Nitrogen Ratio. *Geoderma* 357, 113974. doi:10.1016/j.geoderma.2019.113974
- Korenevsky, A., and Beveridge, T. J. (2007). The Surface Physicochemistry and Adhesiveness of *Shewanella* Are Affected by Their Surface Polysaccharides. *Microbiology-Sgm* 153, 1872–1883. doi:10.1099/mic.0.2006/003814-0
- Kubartová, A., Ranger, J., Berthelin, J., and Beguiristain, T. (2009). Diversity and Decomposing Ability of Saprophytic Fungi from Temperate Forest Litter. *Microb. Ecol.* 58, 98–107. doi:10.1007/s00248-008-9458-8
- Kujawinski, E. B., and Behn, M. D. (2006). Automated Analysis of Electrospray Ionization Fourier Transform Ion Cyclotron Resonance Mass Spectra of Natural Organic Matter. *Anal. Chem.* 78, 4363–4373. doi:10.1021/ac0600306
- Kujawinski, E. B., Longnecker, K., Blough, N. V., Vecchior, R. D., Finlay, L., Kitzner, J. B., et al. (2009). Identification of Possible Source Markers in Marine Dissolved Organic Matter Using Ultrahigh Resolution Mass Spectrometry. *Geochimica Cosmochimica Acta* 73, 4384–4399. doi:10.1016/j.gca.2009.04.033

- Kuzyakov, Y., and Blagodatskaya, E. (2015). Microbial hotspots and hot moments in soil: Concept & review. *Soil Biology and Biochemistry* 83, 184–199.
- Lavallee, J. M., Soong, J. L., and Cotrufo, M. F. (2020). Conceptualizing Soil Organic Matter into Particulate and Mineral-associated Forms to Address Global Change in the 21st Century. *Glob. Change Biol.* 26, 261–273. doi:10.1111/gcb.14859
- Lawrence, C. R., Neff, J. C., and Schimel, J. P. (2009). Does Adding Microbial Mechanisms of Decomposition Improve Soil Organic Matter Models? A Comparison of Four Models Using Data from a Pulsed Rewetting Experiment. *Soil Biol. Biochem.* 41, 1923–1934. doi:10.1016/j.soilbio.2009.06.016
- Lehmann, J., and Kleber, M. (2015). The Contentious Nature of Soil Organic Matter. *Nature* 528, 60–68. doi:10.1038/nature16069
- Lepieux, C., Turpault, M. P., Oger, P., Frey-Klett, P., and Uroz, S. (2012). Correlation of the Abundance of Betaproteobacteria on Mineral Surfaces with Mineral Weathering in Forest Soils. *Appl. Environ. Microbiol.* 78, 7114–7119. doi:10.1128/aem.00996-12
- Li, Y., Zhang, T., Zhou, Y., Zou, X., Yin, Y., Li, H., et al. (2021). Ectomycorrhizal Symbioses Increase Soil Calcium Availability and Water Use Efficiency of Quercus Acutissima Seedlings under Drought Stress. *Eur. J. For. Res.* 140, 1039–1048. doi:10.1007/s10342-021-01383-y
- Liang, C., Amelung, W., Lehmann, J., and Kästner, M. (2019). Quantitative Assessment of Microbial Necromass Contribution to Soil Organic Matter. *Glob. Change Biol.* 25, 3578–3590. doi:10.1111/gcb.14781
- Lützw, M. V., Kögel-Knabner, I., Ekschmitt, K., Matzner, E., Guggenberger, G., Marschner, B., et al. (2006). Stabilization of Organic Matter in Temperate Soils: Mechanisms and Their Relevance under Different Soil Conditions - a Review. *Eur. J. Soil Sci.* 57, 426–445. doi:10.1111/j.1365-2389.2006.00809.x
- Madsen, I. C., and Scarlett, N. V. Y. (2008). "Chapter 11 Quantitative Phase Analysis," in *Powder Diffraction: Theory and Practice*. The Royal Society of Chemistry, 298–331.
- Makarov, M. I. (2019). The Role of Mycorrhiza in Transformation of Nitrogen Compounds in Soil and Nitrogen Nutrition of Plants: A Review. *Eurasian Soil Sc.* 52, 193–205. doi:10.1134/s1064229319020108
- McDonald, D., Price, M. N., Goodrich, J., Nawrocki, E. P., Desantis, T. Z., Probst, A., et al. (2012). An Improved Greengenes Taxonomy with Explicit Ranks for Ecological and Evolutionary Analyses of Bacteria and Archaea. *Isme J.* 6, 610–618. doi:10.1038/ismej.2011.139
- McMurdie, P. J., and Holmes, S. (2013). Phyloseq: An R Package for Reproducible Interactive Analysis and Graphics of Microbiome Census Data. *Plos One* 8, e61217. doi:10.1371/journal.pone.0061217
- Mendes, R., Garbeva, P., and Raaijmakers, J. M. (2013). The rhizosphere microbiome: significance of plant beneficial, plant pathogenic, and human pathogenic microorganisms. *FEMS Microbiology Reviews* 37, 634–663.
- Newcomb, C. J., Qafoku, N. P., Grate, J. W., Bailey, V. L., and De Yoreo, J. J. (2017). Author Correction: Developing a Molecular Picture of Soil Organic Matter-Mineral Interactions by Quantifying Organo-Mineral Binding. *Nat. Commun.* 8, 2017. doi:10.1038/s41467-017-02125-8
- Olayemi, O. P., Kallenbach, C. M., and Wallenstein, M. D. (2022). Distribution of Soil Organic Matter Fractions Are Altered with Soil Priming. *Soil Biol. Biochem.* 164, 108494. doi:10.1016/j.soilbio.2021.108494
- Ozlu, E., and Arriaga, F. (2021). The Role of Carbon Stabilization and Minerals on Soil Aggregation in Different Ecosystems. *Catena* 202, 105303. doi:10.1016/j.catena.2021.105303
- Pett-Ridge, J., and Firestone, M. K. (2017). Using Stable Isotopes to Explore Root-Microbe-Mineral Interactions in Soil. *Rhizosphere* 3, 244–253. doi:10.1016/j.rhisph.2017.04.016
- Phillips, L. A., Ward, V., and Jones, M. D. (2014). Ectomycorrhizal Fungi Contribute to Soil Organic Matter Cycling in Sub-boreal Forests. *Isme J.* 8, 699–713. doi:10.1038/ismej.2013.195
- Possinger, A. R., Zachman, M. J., Enders, A., Levin, B. D. A., Muller, D. A., Kourkoutis, L. F., et al. (2020). Organo-organic and Organo-Mineral Interfaces in Soil at the Nanometer Scale. *Nat. Commun.* 11, 6103. doi:10.1038/s41467-020-19792-9
- Price, J. R., and Velbel, M. A. (2014). Rates of Biotite Weathering, and Clay Mineral Transformation and Neof ormation, Determined from Watershed Geochemical Mass-Balance Methods for the Coweeta Hydrologic Laboratory, Southern Blue Ridge Mountains, North Carolina, USA. *Aquat. Geochem* 20, 203–224. doi:10.1007/s10498-013-9190-y
- Qafoku, N. P. (2015). Climate-Change Effects on Soils: Accelerated Weathering, Soil Carbon, and Elemental Cycling. *Adv. Agron.* 131, 111–172. doi:10.1016/bs.agron.2014.12.002
- Raczka, N. C., Piñeiro, J., Tfaily, M. M., Chu, R. K., Lipton, M. S., Pasa-Tolic, L., et al. (2021). Interactions between Microbial Diversity and Substrate Chemistry Determine the Fate of Carbon in Soil. *Sci. Rep.* 11, 19320. doi:10.1038/s41598-021-97942-9
- Rognes, T., Flouri, T., Nichols, B., Quince, C., and Mahé, F. (2016). VSEARCH: a Versatile Open Source Tool for Metagenomics. *PeerJ* 4, e2584. doi:10.7717/peerj.2584
- Schoch, C. L., Crous, P. W., Groenewald, J. Z., Boehm, E. W. A., Burgess, T. I., De Gruyter, J., et al. (2009). A class-wide phylogenetic assessment of Dothideomycetes. *Studies in Mycology* 64, 1–15.
- Schurig, C., Smittenberg, R., Berger, J., Kraft, F., Woche, S., Goebel, M.-O., et al. (2012). Microbial cell-envelope fragments and the formation of soil organic matter: A case study from a glacier forefield. *Biogeochemistry* 113.
- Shah, F., Nicolás, C., Bentzer, J., Ellström, M., Smits, M., Rineau, F., et al. (2016). Ectomycorrhizal Fungi Decompose Soil Organic Matter Using Oxidative Mechanisms Adapted from Saprotrophic Ancestors. *New Phytol.* 209, 1705–1719. doi:10.1111/nph.13722
- Shi, Z., Balogh-Brunstad, Z., Grant, M., Harsh, J., Gill, R., Thomashow, L., et al. (2014). Cation Uptake and Allocation by Red Pine Seedlings under Cation-Nutrient Stress in a Column Growth Experiment. *Plant Soil* 378, 83–98. doi:10.1007/s11104-013-2016-2
- Simon, A., Hervé, V., Al-Dourobi, A., Verrecchia, E., and Junier, P. (2017). An in situ inventory of fungi and their associated migrating bacteria in forest soils using fungal highway columns. *FEMS Microbiol Ecol* 93.
- Smits, M. M., and Wallander, H. (2017). "Role of Mycorrhizal Symbiosis in Mineral Weathering and Nutrient Mining from Soil Parent Material," in *Mycorrhizal Mediation of Soil*. Editors N. C. Johnson, C. Gehring, and J. Jansa (Amsterdam, Netherlands: Elsevier), 35–46. doi:10.1016/b978-0-12-804312-7.00003-6
- Sokol, N. W., and Bradford, M. A. (2019). Microbial Formation of Stable Soil Carbon Is More Efficient from Belowground than Aboveground Input. *Nat. Geosci.* 12, 46, 53–+.doi:10.1038/s41561-018-0258-6
- Soudzilovskaia, N. A., Van Bodegom, P. M., Terrer, C., Zelfde, M. V., Mccallum, I., Luke McCormack, M., et al. (2019). Global Mycorrhizal Plant Distribution Linked to Terrestrial Carbon Stocks. *Nat. Commun.* 10, 5077. doi:10.1038/s41467-019-13019-2
- Spaccini, R., Piccolo, A., Conte, P., Haberhauer, G., and Gerzabek, M. H. (2002). Increased soil organic carbon sequestration through hydrophobic protection by humic substances. *Soil Biology and Biochemistry* 34, 1839–1851.
- Sposito, G., Skipper, N. T., Sutton, R., Park, S.-H., Soper, A. K., and Greathouse, J. A. (1999). Surface geochemistry of the clay minerals. *Proceedings of the National Academy of Sciences* 96, 3358–3364.
- Sun, Q., Liu, X., Wang, S., and Lian, B. (2020). Effects of mineral substrate on ectomycorrhizal fungal colonization and bacterial community structure. *Sci Total Environ* 721, 137663.
- Taylor, L. L., Leake, J. R., Quirk, J., Hardy, K., Banwart, S. A., and Beerling, D. J. (2009). Biological weathering and the long-term carbon cycle: integrating mycorrhizal evolution and function into the current paradigm. *Geobiology* 7, 171–191.
- Tfaily, M. M., Chu, R. K., Toyoda, J., Tolić, N., Robinson, E. W., Paša-Tolić, L., et al. (2017). Sequential Extraction Protocol for Organic Matter from Soils and Sediments Using High Resolution Mass Spectrometry. *Anal. Chim. Acta* 972, 54–61. doi:10.1016/j.aca.2017.03.031
- Tfaily, M. M., Cooper, W. T., Kostka, J. E., Chanton, P. R., Schadt, C. W., Hanson, P. J., et al. (2014). Organic Matter Transformation in the Peat Column at Marcell Experimental Forest: Humification and Vertical Stratification. *J. Geophys. Res. Biogeosci.* 119, 661–675. doi:10.1002/2013jg002492
- Totsche, K. U., Amelung, W., Gerzabek, M. H., Guggenberger, G., Klumpp, E., Knief, C., et al. (2018). Microaggregates in Soils. *J. Plant Nutr. Soil Sci.* 181, 104–136. doi:10.1002/jpln.201600451
- Turpault, M.-P., Nys, C. C., and Calvaruso, C. C. (2009). Rhizosphere Impact on the Dissolution of Test Minerals in a Forest Ecosystem. *Geoderma* 153, 147–154.

- Vieira, S., Sikorski, J., Gebala, A., Boeddinghaus, R.S., Marhan, S., Rennert, T., et al. (2020). Bacterial colonization of minerals in grassland soils is selective and highly dynamic. *Environ Microbiol* 22, 917–933.
- Uroz, S., Calvaruso, C., Turpault, M. P., Sarniguet, A., De Boer, W., Leveau, J. H. J., et al. (2009). Efficient Mineral Weathering Is a Distinctive Functional Trait of the Bacterial Genus *Collimonas*. *Soil Biol. Biochem.* 41, 2178–2186. doi:10.1016/j.soilbio.2009.07.031
- Uroz, S., Kelly, L. C., Turpault, M.-P., Lepleux, C., and Frey-Klett, P. (2015). The Mineralosphere Concept: Mineralogical Control of the Distribution and Function of Mineral-associated Bacterial Communities. *Trends Microbiol.* 23, 751–762. doi:10.1016/j.tim.2015.10.004
- Wallander, H., Hagerberg, D., and Aberg, G. (2006). Uptake of ⁸⁷Sr from Microcline and Biotite by Ectomycorrhizal Fungi in a Norway Spruce Forest. *Soil Biol. Biochem.* 38, 2487–2490. doi:10.1016/j.soilbio.2006.02.002
- Wallander, H., Nilsson, L. O., Hagerberg, D., and Bååth, E. (2001). Estimation of the Biomass and Seasonal Growth of External Mycelium of Ectomycorrhizal Fungi in the Field. *New Phytol.* 151, 753–760. doi:10.1046/j.0028-646x.2001.00199.x
- White, R. A., Rivas-Ubach, A., Borkum, M. I., Köberl, M., Bilbao, A., Colby, S. M., et al. (2017). The State of Rhizospheric Science in the Era of Multi-Omics: A Practical Guide to Omics Technologies. *Rhizosphere* 3, 212–221. doi:10.1016/j.rhisp.2017.05.003
- White, T. J., Bruns, T., Lee, S., and Taylor, J. (1990). “Amplification and Direct Sequencing of Fungal Ribosomal Rna Genes for Phylogenetics.” in *PCR Protocols*. Editors M. A. Innis, D. H. Gelfand, J. J. Sninsky, and T. J. White (San Diego: Academic Press), 315–322. doi:10.1016/b978-0-12-372180-8.50042-1
- Whitman, T., Neurath, R., Perera, A., Chu-Jacoby, I., Ning, D., Zhou, J., et al. (2018). Microbial Community Assembly Differs across Minerals in a Rhizosphere Microcosm. *Environ. Microbiol.* 20, 4444–4460. doi:10.1111/1462-2920.14366
- Wieder, W. R., Bonan, G. B., and Allison, S. D. (2013). Global Soil Carbon Projections Are Improved by Modelling Microbial Processes. *Nat. Clim. Change* 3, 909–912. doi:10.1038/nclimate1951
- Wieder, W. R., Grandy, A. S., Kallenbach, C. M., and Bonan, G. B. (2014). Integrating Microbial Physiology and Physio-Chemical Principles in Soils with the Microbial-Mineral Carbon Stabilization (MIMICS) Model. *Biogeosciences* 11, 3899–3917. doi:10.5194/bg-11-3899-2014
- Willemsen, J.A.R., Myneni, S.C.B., and Bourg, I.C. (2019). Molecular Dynamics Simulations of the Adsorption of Phthalate Esters on Smectite Clay Surfaces. *The Journal of Physical Chemistry C* 123, 13624–13636.
- Conflict of Interest:** The authors declare that the research was conducted in the absence of any commercial or financial relationships that could be construed as a potential conflict of interest.
- Publisher’s Note:** All claims expressed in this article are solely those of the authors and do not necessarily represent those of their affiliated organizations, or those of the publisher, the editors and the reviewers. Any product that may be evaluated in this article, or claim that may be made by its manufacturer, is not guaranteed or endorsed by the publisher.
- Copyright © 2022 Dohnalkova, Tfairly, Chu, Smith, Brislawn, Varga, Crump, Kovarik, Thomashow, Harsh, Keller and Balogh-Brunstad. This is an open-access article distributed under the terms of the Creative Commons Attribution License (CC BY). The use, distribution or reproduction in other forums is permitted, provided the original author(s) and the copyright owner(s) are credited and that the original publication in this journal is cited, in accordance with accepted academic practice. No use, distribution or reproduction is permitted which does not comply with these terms.